The Plant Cell, Vol. 30: 2677–2703, November 2018, www.plantcell.org © 2018 ASPB.

BREAKTHROUGH REPORT

A Ycf2-FtsHi Heteromeric AAA-ATPase Complex Is Required for Chloroplast Protein Import[OPEN]

Shingo Kikuchi,[a,1] Yukari Asakura,[a,1] Midori Imai,[a] Yoichi Nakahira,[b] Yoshiko Kotani,[a] Yasuyuki Hashiguchi,[c] Yumi Nakai,[d] Kazuaki Takafuji,[e] Jocelyn Bédard,[a] Yoshino Hirabayashi-Ishioka,[a] Hitoshi Mori,[f] Takashi Shiina,[g] and Masato Nakai[a,2]

[a]Institute for Protein Research, Osaka University, Osaka 565-0871, Japan
[b]College of Agriculture, Ibaraki University, Ami-cho, Inashiki, Ibaraki 300-0393, Japan
[c]Department of Biology, Osaka Medical College, Takatsuki, Osaka 569-8686, Japan
[d]Department of Biochemistry, Osaka Medical College, Takatsuki, Osaka 569-8686, Japan
[e]CoMIT Omics Center, Graduate School of Medicine, Osaka University, Osaka 565-0871, Japan
[f]Graduate School of Bioagricultural Sciences, Nagoya University, Furo-cho, Chikusa-ku, Nagoya, Aichi 464-8601, Japan
[g]School of Human Environment Science, Kyoto Prefectural University, Sakyo-ku, Kyoto 606-8522, Japan

ORCID IDs: 0000-0001-9033-6242 (S.K.); 0000-0002-8689-5049 (Y.A.); 0000-0002-3294-9646 (M.I.); 0000-0003-2582-2310 (Y.N.); 0000-0002-2359-138X (Y.K.); 0000-0003-4706-5269 (Y.H.); 0000-0001-6785-4789 (Y.N.); 0000-0001-6417-8156 (K.T.); 0000-0003-3204-0122 (J.B.); 0000-0002-4522-9365 (Y.H.-I.); 0000-0001-7331-0884 (H.M.); 0000-0002-5522-1535 (T.S.); 0000-0003-4744-9916 (M.N.)

Chloroplasts import thousands of nucleus-encoded preproteins synthesized in the cytosol through the TOC and TIC translocons on the outer and inner envelope membranes, respectively. Preprotein translocation across the inner membrane requires ATP; however, the import motor has remained unclear. Here, we report that a 2-MD heteromeric AAA-ATPase complex associates with the TIC complex and functions as the import motor, directly interacting with various translocating preproteins. This 2-MD complex consists of a protein encoded by the previously enigmatic chloroplast gene *ycf2* and five related nuclear-encoded FtsH-like proteins, namely, FtsHi1, FtsHi2, FtsHi4, FtsHi5, and FtsH12. These components are each essential for plant viability and retain the AAA-type ATPase domain, but only FtsH12 contains the zinc binding active site generally conserved among FtsH-type metalloproteases. Furthermore, even the FtsH12 zinc binding site is dispensable for its essential function. Phylogenetic analyses suggest that all AAA-type members of the Ycf2/FtsHi complex including Ycf2 evolved from the chloroplast-encoded membrane-bound AAA-protease FtsH of the ancestral endosymbiont. The Ycf2/FtsHi complex also contains an NAD-malate dehydrogenase, a proposed key enzyme for ATP production in chloroplasts in darkness or in nonphotosynthetic plastids. These findings advance our understanding of this ATP-driven protein translocation system that is unique to the green lineage of photosynthetic eukaryotes.

INTRODUCTION

Most nuclear-encoded chloroplast preproteins are biosynthesized in the cytosol as a larger preprotein with an N-terminal transit peptide, then translocated across the outer and inner envelope membranes via protein translocons called TOC (translocon on the outer chloroplast membrane) and TIC (translocon on the inner chloroplast membrane), respectively (Jarvis and López-Juez, 2013; Nakai, 2015a; Paila et al., 2015). The preproteins are initially recognized by the TOC receptor proteins, namely, Toc159 and/or Toc33/Toc34, and pass through a β-barrel channel protein, Toc75, into the intermembrane space. GTP binding to TOC receptors facilitates or triggers this translocation. Subsequently, the preproteins are translocated across the inner envelope membrane through the TIC complex, driven by energy derived from ATP hydrolysis. A predicted but unidentified import motor ATPase associated with the TIC complex is believed to provide an ATP-derived pulling force from the stromal side of the inner envelope membrane to drive preprotein translocation (Theg et al., 1989; Shi and Theg, 2013).

Whereas a consensus has been established regarding the TOC complex components, there remains debate about the molecular identities of the TIC components, as well as the associated import motor. The classical model involves Tic110 and Tic40 as central components of TIC, with stromal molecular chaperones, particularly Hsp70 and Hsp93 (ClpC), playing crucial roles in the ATP-dependent translocation of the preproteins across the inner envelope membrane (Nielsen et al., 1997; Su and Li, 2010; Liu et al., 2014; Flores-Pérez et al., 2016; Huang et al., 2016). Other

[1]These authors contributed equally to this work.
[2]Address correspondence to nakai@protein.osaka-u.ac.jp.
The author responsible for distribution of materials integral to the findings presented in this article in accordance with the policy described in the Instructions for Authors (www.plantcell.org) is: Masato Nakai (nakai@protein.osaka-u.ac.jp).
[OPEN]Articles can be viewed without a subscription.
www.plantcell.org/cgi/doi/10.1105/tpc.18.00357

stromal chaperones, Hsp90C and Cpn60, have also been found to be associated with the preprotein import process (Kessler and Blobel, 1996; Inoue et al., 2013).

Recently, using transgenic *Arabidopsis thaliana* plants expressing a tagged-form of Tic20, another key component of TIC, we identified a 1-MD complex on the inner envelope membrane consisting of Tic20/Tic56/Tic100/Tic214 (Kikuchi et al., 2009, 2013). Tic214 is encoded by the chloroplast gene *ycf1* (Nakai, 2015b). We further established a pivotal role for Tic214 in a major TIC channel complex translocating preproteins across the inner envelope membrane and thus proposed an extensively revised model for the TIC translocation system (Kikuchi et al., 2013; Nakai, 2015a, 2018). Since then, the molecular identity of the factor(s) that cooperate with the newly identified TIC complex and function as an import motor to couple ATP hydrolysis to preprotein translocation has remained an intriguing question. Most previous studies considered these identities in the context of the above-mentioned classical candidate TIC components, namely, Tic110 and Tic40 (Richardson et al., 2017), neither of which could be confirmed to interact with the Tic20/Tic56/Tic100/Tic214(Ycf1) complex or the translocating preproteins (Kikuchi et al., 2009, 2013).

In this study, we aimed to identify an import motor that physically and functionally cooperates with the Tic20/Tic56/Tic100/Tic214(Ycf1) TIC complex. We discovered a previously unidentified 2-MD inner envelope membrane-bound AAA-ATPase (adenosine triphosphatases associated with diverse cellular activities) complex that plays a pivotal role as a TIC-associated import motor. The import motor complex likely originated from the ancestral membrane-bound hexameric protease FtsH, which consists of an AAA-ATPase domain and a zinc protease domain and is known to play a key quality control role in degrading misassembled and damaged membrane proteins in bacteria (Okuno and Ogura, 2013).

RESULTS

Evolutionary Relationships among the Inner Envelope AAA-Type ATPase Ycf2 and FtsHi Proteins

In addition to the well-known stromal molecular chaperones, including Hsp70 and Hsp93 (ClpC), inner envelope-localized AAA-type ATPases have been detected in proteomic analyses of the chloroplasts (Sun et al., 2009; Ferro et al., 2010). Among these is Ycf2, encoded by an enigmatic large open reading frame in green-lineage chloroplast genomes (Figure 1A). The chloroplast proteomes also contained five nucleus-encoded proteins similar to the bacterial membrane-bound AAA metalloprotease FtsH but lacking the zinc binding motif (His-Glu-Xaa-Xaa-His) essential for proteolytic activity. These proteins were therefore called FtsHi proteins (FtsH-inactive) and are named FtsHi1, FtsHi2, FtsHi3, FtsHi4, and FtsHi5 (Figure 1A) (Sokolenko et al., 2002; Wagner et al., 2012).

We first examined the origin of Ycf2, finding that while most green lineages, including the land plants and green algae such as *Chlamydomonas reinhardtii*, possess fairly long chloroplast-encoded Ycf2 proteins with no zinc binding motif, the *Mesostigma* and *Chlorokybus* chloroplast genomes encode short Ycf2 proteins that have clear sequence similarity to cyanobacterial FtsH and still possess an incomplete zinc binding motif relict (Figure 1C). The chloroplast genome of *Rhodophyta*, a basal lineage, retains a gene encoding an FtsH ortholog containing the complete zinc binding motif. It can therefore be concluded that chloroplast *ycf2* originates from a chloroplast gene, *ftsH*, of endosymbiotic origin and that the zinc binding motif was lost and the protein size increased during the evolution of the green lineage.

We then constructed a phylogenetic tree to clarify the evolutionary relationship between the FtsHi and Ycf2 proteins and cyanobacterial/*Rhodophyta* FtsH1 and FtsH2. Because their N-terminal segments containing transmembrane domains vary in length and sequence, we aligned the C-terminal sequences starting from the Walker A motif of various FtsH-like proteins and Ycf2 proteins (Supplemental File 1); FtsHi3 was excluded because of its very short C-terminal domain. We used two different methods to construct the tree: the Bayesian approach and the maximum likelihood method. In both cases, although the node from which Ycf2 diverged remained uncertain, in land plants, Ycf2 and respective FtsHi proteins form monophyletic groups (Supplemental Figures 1 and 2). The land plant FtsH12 protein, which retains the zinc binding motif (Figure 1A), was also included in this clade but likely absent in the *Chlorophyta*. Hydrophobic residues at the pore loop located between the Walker A and B motifs, which are known to grip substrate polypeptides upon their translocation through the hexameric FtsH ring, were well conserved in FtsHi1, FtsHi2, FtsHi3, FtsHi4, and FtsHi5, but not in FtsH12, whereas the corresponding region of Ycf2 contained a long acidic insertion. It should be further noted that *ycf2* shares a similar evolutionary history with another chloroplast gene, *ycf1*, which encodes a key component Tic214 of the TIC complex (Kikuchi et al., 2013; Nakai, 2015b, 2018). Both *ycf1* and *ycf2* seem to have undergone a synchronized and drastic extension during the evolution of the green lineages (Figure 1C; see Discussion for details; Kikuchi et al., 2013; Nakai, 2015b, 2018).

Association of Evolutionary-Related Ycf2 and FtsH-Like Proteins with Various Translocation Intermediates

We investigated whether the inner envelope-localized AAA-type ATPases with currently unknown functions, namely, the FtsHi proteins, FtsH12, and Ycf2, interact with translocating preproteins using in vitro import reactions with intact chloroplasts isolated from Arabidopsis. For this purpose, we utilized a highly specific method that we developed previously (Figure 2A; Kikuchi et al., 2013; Nakai, 2015a, 2015b). We introduced a tobacco etch virus (TEV) protease cleavage site followed by a Protein A-tag at the C terminus of the model preproteins. The in vitro import reactions were performed using these purified Protein A-tagged model preproteins and isolated Arabidopsis chloroplasts in the presence or absence of ATP. After solubilization with a mild detergent, digitonin, to preserve the translocation intermediate complexes, the model preproteins and any associated proteins were purified using immunoglobulin G (IgG)-Sepharose and specifically eluted by TEV cleavage under nondenaturing

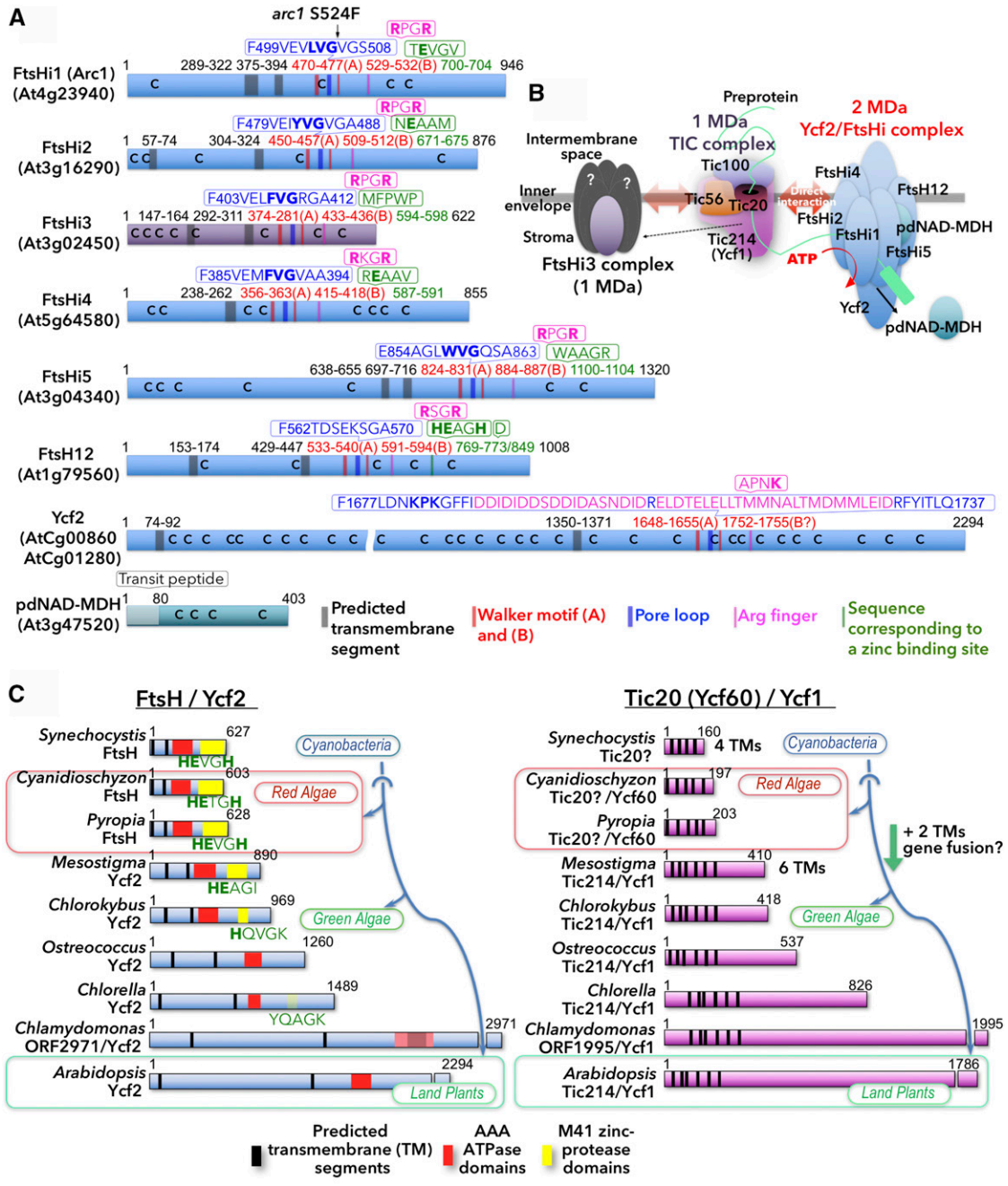

Figure 1. The Plastome-Encoded AAA Protein Ycf2 and Evolutionarily Related FtsH-Like Proteins.

(A) Schematic presentation of the Ycf2/FtsHi complex components and FtsHi3 from Arabidopsis. Positions of predicted transmembrane domains (gray), the Walker motifs (red), the pore loop (blue), the Arg finger (magenta), the zinc binding region (green), and Cys residues (C) are depicted. Amino acid sequences corresponding to the pore loop region and the zinc binding region are shown.

(B) Inferred model (deduced by this study) of the 2-MD Ycf2/FtsHi complex function in preprotein translocation across the inner envelope membrane of chloroplasts as a TIC-associated import motor.

(C) Coevolution of chloroplast-encoded FtsH/Ycf2 and Tic20 (Ycf60)/Tic214 (Ycf1) of cyanobacterial origin. Schematic representation of size expansion of chloroplast genome-encoded Ycf2 (upper) and Tic214 (Ycf1; lower) proteins along with the evolution of red and green lineages from their most probable ancestral proteins encoded by the cyanobacterial genomes. It should be noted that the zinc binding motif (HEXXH) critical for protease activity of FtsH-type metalloprotease appears to have been gradually lost from Ycf2 proteins during evolution. Sequences from NCBI (http://www.ncbi.nlm.nih.gov/protein): *Synechocystis* FtsH (BAA10230), *Cyanidioschyzon* FtsH (BAC76202), *Pyropia* FtsH (AGH27655), *Mesostigma* Ycf2 (AAF43852), *Chlorokybus* Ycf2 (ABD62184), *Ostreococcus* Ycf2 (CAL36342), *Chlorella* Ycf2 (ADZ04994), Chlamydomonas Ycf2 (ACJ50152), Arabidopsis Ycf2 (BAA84428), *Synechocystis* Tic20 homolog (BAA17427), *Cyanidioschyzon* Tic20/Ycf60 (BAC76161), *Pyropia* Tic20/Ycf60 (AGH27688), *Mesostigma* Ycf1 (AAF43878), *Chlorokybus* Ycf1 (ABD62257), *Ostreococcus* Ycf1 (CAL36331), *Chlorella* Ycf2 (ADZ05009), Chlamydomonas Ycf1 (CAA63385) (Boudreau et al., 1997), and Arabidopsis Ycf1 (BAA84445).

conditions. Immunoblot analyses were used to assess the specific associations of the various candidate proteins. This purification/identification method relies on the highly specific and strong association between the introduced Protein A-tag of the preproteins and the IgG-Sepharose, but does not require any prior chemical cross-linking or the use of different polyclonal antibodies for each candidate component. It can therefore minimize the false positives associated with the detection of abundant or nonspecific proteins as preprotein-associating factors.

Using this method, we found that, depending on the presence of ATP during import reactions, Ycf2, FtsHi1, FtsHi2, FtsHi4, FtsHi5, and FtsH12 were significantly associated with the translocation intermediates of the model preprotein pFd (ferredoxin; pFd-TEV-ProtA) (Figure 2B). Importantly, Toc159/Toc75 and Tic214/Tic100 were also found to be associated with the translocating preprotein. We did not observe any association between FtsHi3 and the tagged preprotein. Moreover, no significant specific associations were observed between the translocating preprotein and stromal Hsp70, Hsp93 (ClpC), the classical Tic protein Tic110, Tic40, or Var2, a thylakoid FtsH homolog.

We further tested the interactions of the proteins with various model preproteins, including pSSU (Rubisco small subunit; pSSU-TEV-ProtA), pL11 (ribosomal protein L11; pL11*-TEV-ProtA), as well as pLHCP (light-harvesting chlorophyll binding protein; pLHCP*-TEV-ProtA; * indicates the presence of a FLAG tag) (Supplemental Figure 3). These model preproteins gave similar results to those obtained with pFd-TEV-ProtA, except for FtsHi3; Ycf2, FtsHi1, FtsHi2, FtsHi4, FtsHi5, and FtsH12 were all specifically associated with translocating preproteins as were Toc159/Toc75 and Tic214/Tic100, whereas no association between the preproteins and Hsp70, Hsp93 (ClpC), Tic110, or Tic40 were observed. FtsHi3 did not associate with the translocating pFd-TEV-Protein A (Figure 2B), but did associate with pSSU, pL11, and pLHCP (Supplemental Figure 3).

We then explored whether the observed associations with these preproteins are specific to the proteins being translocated across the inner envelope membrane, but not required for outer envelope-localized proteins. To this end, we constructed a model outer envelope-localized protein OEP7*-TEV-Protein A (OEP7*-TEV-ProtA). We confirmed the integration of a certain proportion of the added OEP7 fusion protein into the envelope membranes after incubation with isolated and alkaline-treated intact chloroplasts at 25°C for 20 min (Figure 2C). Ycf2, FtsHi2, and FtsH12 did not associate with OEP7*-TEV-ProtA during its integration into the outer envelope membrane (Figure 2D). Thus, the transient associations with Ycf2 and FtsHi/FtsH12 proteins are specific to preproteins destined to be translocated across the inner envelope membrane.

FtsHi1, FtsHi2, FtsHi4, FtsHi5, FtsH12, and Ycf2 Form a 2-MD Complex with pdNAD-MDH at the Inner Envelope Membrane

AAA-type proteins generally exist as a homo- or heterohexamers (White and Lauring, 2007). Using blue-native (BN)-PAGE for the analysis of 1% Triton X-100-solubilized Arabidopsis chloroplasts, we found that FtsHi1, FtsHi2, FtsHi4, FtsHi5, Ycf2, and FtsH12 comigrated at ~2 MD, whereas FtsHi3 was present in a distinct ~1-MD complex, and a similar 2-MD complex likely exists in tobacco (*Nicotiana tabacum*) (Figures 3A and 3B). We next investigated whether Ycf2 forms a 2-MD complex with FtsHi1, FtsHi2, FtsHi4, FtsHi5, and FtsH12 in tobacco. We modified the 3′ end of the tobacco chloroplast gene *ycf2* to encode a Ycf2 protein with a HA tag at the C terminus and confirmed an almost homoplasmic replacement of *ycf2* with the modified gene by genomic PCR (Supplemental Figures 4A and 4B, upper panels). We also constructed a HA-tagged version of the tobacco chloroplast gene *ycf1* encoding Tic214 (Supplemental Figures 4A and 4B, lower panels). We selected the Y2C-11(Y2C) and Y1C-3(Y1C) transplastomic lines expressing the HA tagged-Ycf2 and the HA-tagged Ycf1 (Tic214), respectively, for further study. In tobacco, both *ycf1* and *ycf2* were previously demonstrated to be indispensable (Drescher et al., 2000). Both the Y1C and Y2C lines grew similarly to the wild-type parental line (Figure 3C), indicating that the introduced HA-tag does not disturb the function of these proteins. Because we modified these genes only at their 3′ ends, their expressions were expected to be under the control of their authentic promoters. This enabled us to directly compare the protein expression levels between Ycf1 (Tic214)-HA and Ycf2-HA using an immunoblot analysis of chloroplast extracts with the anti-HA-tag antibody. As shown in Figure 3D, slightly higher (~2-fold) levels of Ycf1 (Tic214) than Ycf2 were observed.

Using the established transgenic plants, we purified the Ycf2-HA-containing complex in the presence of 1% Triton X-100 and 300 mM NaCl. The purified Ycf2-HA complex retained its 2-MD size (Figure 3E) and was found to contain six additional protein bands ranging between 32 and 120 kD with similar stoichiometry, five of which were confirmed to be FtsHi1, FtsHi2, FtsHi4, FtsHi5, and FtsH12 using immunoblotting (Figures 3E and 3F). Antibodies raised against the Arabidopsis FtsHi/FtsH12 proteins could specifically recognize the tobacco counterparts, which showed similar electrophoretic mobility with those of Arabidopsis (Supplemental Figure 4C). A liquid chromatography-mass spectrometry/mass spectrometry (LC-MS/MS) analysis revealed that the remaining 32-kD band in the purified Ycf2-HA complex was a mature form of plastidial NAD-malate dehydrogenase (pdNAD-MDH) from tobacco (Figures 1A and 3F; Supplemental Figure 5). The purified 2-MD Ycf2-HA complex had pdNAD-MDH enzyme activity (see Methods). Consistent with previous observations (Cvetić et al., 2008; Sun et al., 2009; Ferro et al., 2010; Schreier et al., 2018), pdNAD-MDH exists both as a component of the 2-MD complex as well as in a smaller soluble stromal form in Arabidopsis and tobacco (Figures 3A and 3B, respectively). We confirmed that pdNAD-MDH was associated with the various preprotein translocation intermediates as a constituent of the Ycf2/FtsHi complex in Arabidopsis chloroplasts (Figure 2B; Supplemental Figure 3). The inner envelope-localized Ycf2, FtsHi1, FtsHi2, FtsHi4, FtsHi5, FtsH12, and pdNAD-MDH proteins therefore form a stable 2-MD complex (the Ycf2/FtsHi complex), which interacts with the translocating preproteins. A model of Ycf2/FtsHi complex function, inferred from data presented in this study, is shown in Figure 1B.

To investigate the direct interactions of individual Ycf2/FtsHi complex components with translocating preproteins in tobacco

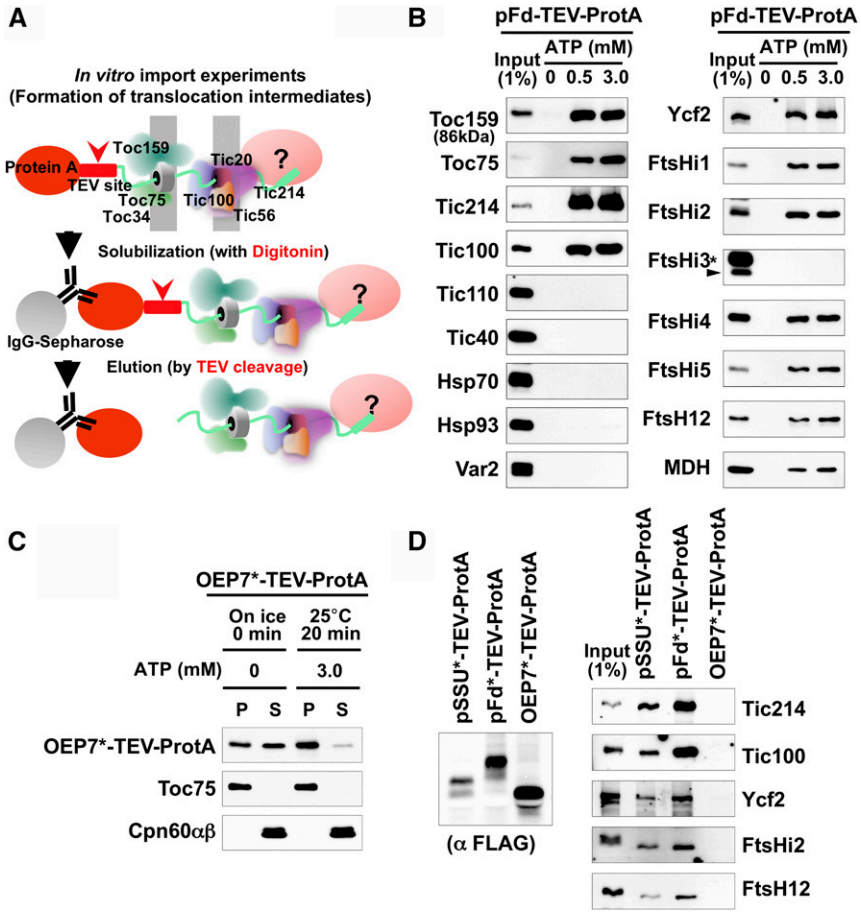

Figure 2. Association of the Ycf2 and FtsH-Like Proteins with a Model Translocating Preprotein together with TOC and TIC Components.

Inferred model of Ycf2/FtsHi complex function.

(A) Schematic diagram showing how translocation intermediate-associating proteins/complexes are purified (Kikuchi et al., 2013). First, we performed in vitro import experiments with isolated Arabidopsis chloroplasts using a purified model preprotein consisting of an entire authentic preprotein containing a transit peptide and a C-terminal Protein A-tag (ProtA; 289 amino acids). A cleavage site of TEV protease (12 amino acids) was introduced in between the preprotein and the Protein A-tag. After import, translocation intermediates were purified after solubilization by digitonin using IgG-Sepharose beads. Bound translocating preprotein-associated proteins were eluted under nondenaturing conditions by TEV cleavage and specifically eluted by TEV cleavage under nondenaturing conditions.

(B) Affinity purification of translocation intermediate complexes via a model preprotein pFd-TEV-ProtA (ferredoxin preprotein, 146 amino acids; TEV-ProtA, 301 amino acids) after in vitro import reactions under indicated ATP concentration (0, 0.5, and 3 mM) with isolated Arabidopsis chloroplasts for 10 min at 25°C. Purification was performed under high-salt conditions (250 mM NaCl) using digitonin as detergent. Association of various chloroplast proteins with the pFd-TEV-ProtA was assessed by immunoblotting using respective specific antibodies. Input lanes contained 1% equivalent of digitonin-solubilized chloroplast extracts used for each purification. Asterisks, cross-reactions to abundant thylakoidal Var2, a typical FtsH homolog. MDH, pdNAD-MDH. Tic110 and Tic40, well-known classical Tic proteins that are not included in the TIC20/56/100/214 complex did not associate at all with translocating pFd-TEV-ProtA.

(C) Insertion of $OEP7_{FLAG}$-TEV-ProteinA (a 7-kD outer envelope membrane protein, 64 amino acids) (OEP7*-TEV-ProtA) into the outer envelope membrane in vitro. The purified OEP7*-TEV-ProtA was incubated with isolated Arabidopsis chloroplasts in the absence of ATP on ice or in the presence of ATP for 20 min at 25°C. After import, chloroplasts were treated by alkaline extraction with 0.1 M Na_2CO_3, pH 11.5, and separated into integral membrane proteins (P) and soluble or peripherally-bound membrane proteins (S) by centrifugation. Integration of OEP*-TEV-ProtA was assessed by immunoblotting using anti-FLAG-tag antibody. Toc75 was also analyzed as an integral membrane protein control whereas Cpn60αβ (chaperonin α and β proteins) as soluble proteins.

(D) Specific binding of the Ycf2/FtsHi complex components to the translocating preproteins, namely, pS*-TEV-ProtA and pFd*-TEV-ProtA, but not to OEP7*-TEV-ProtA. pS*-TEV-ProtA, pFd*-TEV-ProtA, and OEP7*-TEV-ProtA were separately incubated with isolated Arabidopsis chloroplasts in the presence of 0.1 mM ATP (pS*-TEV-ProtA and pFd*-TEV-ProtA) or 3 mM ATP (OEP7*-TEV-ProtA) for 20 min at 25°C. Chloroplasts were reisolated and washed several times and were analyzed by immunoblotting using anti-FLAG tag antibody to confirm the presence of bound preproteins (left panel). After solubilization of chloroplasts by digitonin, preprotein-associating proteins were purified and analyzed as in (**B**, right panel).

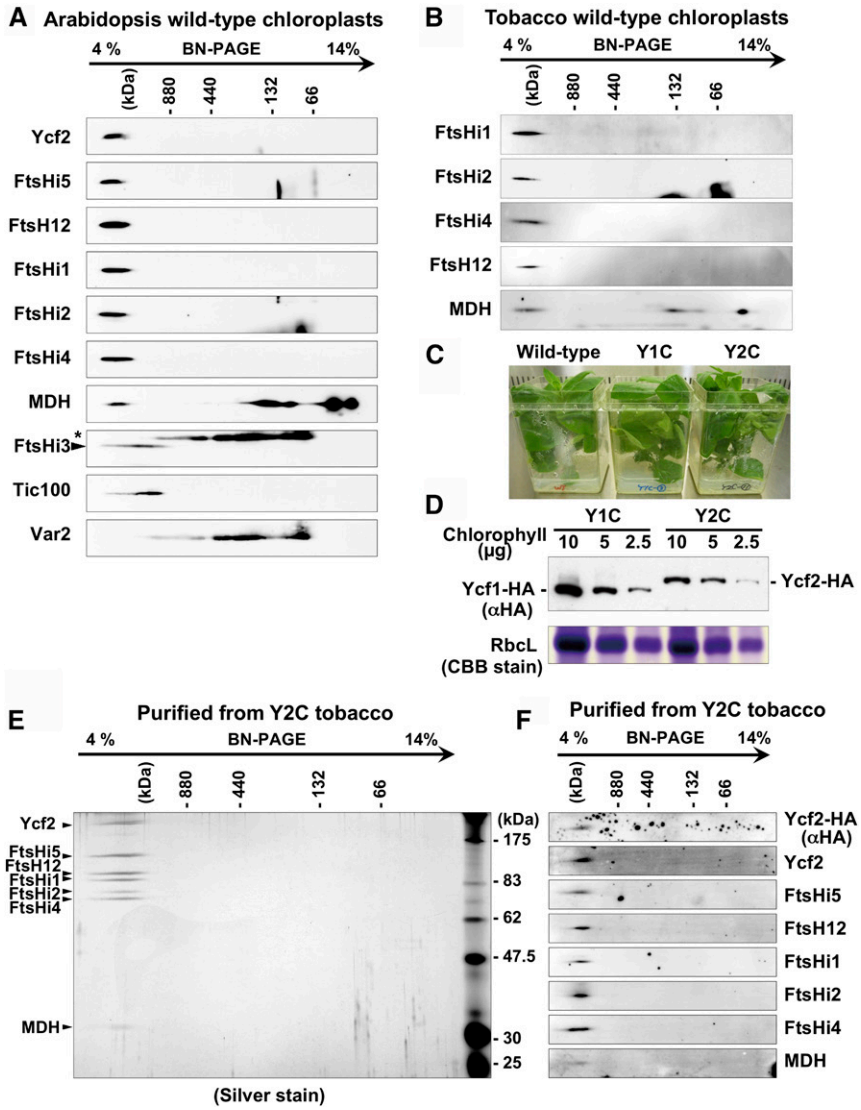

Figure 3. Purification of the 2-MD Ycf2/FtsHi Complex from Transplastomic Tobacco Plants Expressing the C-Terminal HA-Tagged Ycf2 Protein.

(A) Ycf2 and FtsH-like proteins migrate 2-MD area upon BN-PAGE analysis of both Arabidopsis and tobacco chloroplasts. 2D-BN/SDS-PAGE analysis of Arabidopsis chloroplasts followed by immunoblotting. Chloroplasts were solubilized with 1% Triton X-100 in the presence of 300 mM NaCl, and solubilized proteins/complexes were separated by 4 to 14% BN-PAGE as the first dimension and SDS-PAGE as the second dimension followed by immunoblotting using antisera against indicated proteins. MDH, pdNAD-MDH. Asterisk indicates cross-reactions to abundant thylakoidal Var2 (FtsH2).
(B) Isolated tobacco chloroplasts were analyzed as in **(A)**.
(C) Generation of transplastomic tobacco lines expressing C-terminal HA-tagged Ycf2 (Y2C) or Ycf1 (Y1C) proteins. See Supplemental Figure 4 for details. The transplastomic lines (Y2C and Y1C) exhibited normal growth. The Y2C-11 and Y1C-3 lines and their parental tobacco line (Wild-type) were cultivated on MS media containing 3% sucrose for 1 month under the normal growth condition.
(D) Comparison of protein levels of Ycf2-HA and Ycf1-HA proteins is shown. Chloroplasts (equivalents to indicated amounts of chlorophylls) isolated from the Y2C-11 (Y2C) and the Y1C-3 (Y1C) lines were analyzed by SDS-PAGE followed by immunoblotting using anti-HA-tag antibody (upper) or by Coomassie Brilliant Blue (CBB) staining to compare the plastome-encoded Rubisco large subunit protein levels.
(E) The 2-MD Ycf2/FtsHi complex contains five FtsH-like proteins and pdNAD-MDH. The purified 2-MD Ycf2-HA complex analyzed by silver staining. Chloroplasts isolated from the Y2C-11 line were solubilized by 1% Triton X-100 in the presence of 300 mM NaCl and purified using anti-HA-tag agarose beads. Specifically bound proteins were eluted by HA-peptides and analyzed by 2D-BN/SDS-PAGE analysis followed by silver staining. MDH, pdNAD-MDH.
(F) As in **(E)** but after 2D-BN/SDS-PAGE separation, indicated proteins were analyzed by immunoblotting using corresponding antisera raised against Arabidopsis counterparts.

chloroplasts, a chemical cross-linking with DSP (dithiobis[succinimidylpropionate]) was performed after the translocation intermediates were accumulated in an in vitro import into tobacco chloroplasts in the presence of 0.5 mM ATP. We chose pL11*-TEV-ProtA for the cross-linking experiments because of its efficient formation of translocation intermediates (Supplemental Figures 6A and 6B). After the complete dissociation/denaturation of the envelope proteins/complexes with 1% SDS, subsequent pull-down experiments were performed using IgG-Sepharose beads without reducing reagents, then analyzed using SDS-PAGE under reducing conditions to cleave the cross-linker arm, followed by immunoblotting (Supplemental Figure 6C). In addition to the major TOC and TIC components [Toc75, Toc159, and Tic214 (Ycf1-HA)], tobacco Ycf2, FtsHi1, FtsHi2, FtsHi4, and FtsHi5 were all found to have been cross-linked with translocating pL11*-TEV-ProtA. We also detected trace amounts of FtsH12 in the pull-down fraction, suggesting that translocating pL11*-TEV-ProtA interacts with the individual components of the Ycf2/FtsHi complex to some extent. Such interactions were hardly observed for Tic110, Hsp93, or Hsp70 under these experimental conditions. These results clearly indicate that the involvement of the Ycf2/FtsHi complex together with the TOC and TIC complexes in preprotein translocation is not restricted to Arabidopsis but also can be observed in tobacco chloroplasts.

A Stromally Exposed Membrane Topology for the Ycf2/FtsHi Complex Components at the Inner Envelope Membrane

To obtain information regarding the membrane topology of the 2-MD Ycf2/FtsHi complex containing pdNAD-MDH, we performed a thermolysin treatment in combination with a PEG-Mal (polyethylene glycol maleimide) modification on inverted inner envelope membrane vesicles prepared from Arabidopsis chloroplasts (Keegstra and Yousif, 1986) (Supplemental Figure 7A). Both thermolysin and PEG-Mal are membrane-impermeable so only the stromally exposed domains of the proteins could be degraded or modified. Depending on the numbers of covalent modifications made by PEG-Mal, certain size-shifts could be observed in the migrating proteins during SDS-PAGE separation. Tic110, a classical Tic protein, is a good example of an inner envelope membrane protein with a large stromally exposed domain (Jackson et al., 1998). It was completely degraded by thermolysin and modified by PEG-Mal, even without the addition of detergent dodecylmaltoside (Supplemental Figure 7A). This also indicates that there was very little contamination of the inner envelope membrane vesicles by noninverted vesicles. With the exception of pdNAD-MDH, the Ycf2/FtsHi complex components exhibited certain degrees of sensitivity to thermolysin or PEG-Mal modification even in the absence of the detergent, suggesting that most of their C-terminal AAA module-containing domains faced the stroma (Figures 1A and 1B; Supplemental Figure 7A). Membrane-bound pdNAD-MDH showed complete resistance to both treatments even after solubilization with the detergent and thus appeared to be deeply embedded within the complex (Supplemental Figure 7B). This is in marked contrast to the stromally localized pdNAD-MDH, which showed significant sensitivity to both treatments.

The observed membrane topology of the Ycf2/FtsHi complex with stromally exposed AAA-ATPase domains is consistent with the idea that it provides a pulling force for preprotein translocation (Figure 1B) and also with the membrane topology of the ancestral bacterial FtsH proteases, which face the cytoplasm. However, these biochemical assessments of membrane topology have some difficulties or limitations, especially for the components included within a hetero-oligomeric complex; therefore, the precise membrane topology of these complexes should be determined in future structural studies.

The 2-MD Ycf2/FtsHi Complex and the TIC Complex Physically Interact to Form a Supercomplex

When we purified the Ycf2-HA complex from tobacco using the milder detergent dodecylmaltoside and physiological salt concentrations (150 mM NaCl), TIC components such as Tic214 (Ycf1), Tic100, and Tic56 were copurified with the Ycf2/FtsHi complex even in the absence of translocating preproteins (Figure 4A). The association of the TIC complex with the Ycf2/FtsHi complex under low salt conditions was also observed in Arabidopsis (Figure 4B), suggesting that the Ycf2/FtsHi complex and the TIC complex are physically interacting partner complexes and exist to some extent as a supercomplex (Figure 1B). This observation is consistent with the idea that the Ycf2/FtsHi complex acts as a TIC-associated import motor.

High-salt conditions were used to purify the translocation intermediates (Figures 2A and 2B; Supplemental Figure 3). We compared the abundance of the Ycf2/FtsHi complex components copurified using an ATP-dependent arrested translocating preprotein (pFd-TEV-ProtA; Figure 4C, rightmost lane) with the trace amounts that remained associated with the TIC complex purified using tagged-Tic20 under the same high-salt conditions without the addition of preproteins (Figure 4C, purified PA2-TIC) ((Kikuchi et al., 2013). Much higher amounts of the Ycf2/FtsHi complex components were copurified with translocating pFd-TEV-ProtA compared with the basal levels of those components associated with the TIC complex (PA2-TIC) without addition of preproteins. The data shown in Figure 4D confirm that, in the absence of translocating preproteins, the Ycf2/FtsHi complex did not show an increased association with the TIC complex under the high-salt conditions even after incubation in the presence of ATP. These results point to the direct involvement of the Ycf2/FtsHi complex in preprotein translocation.

LC-MS/MS Analysis of Translocation Intermediates Suggests the Formation of TOC-TIC-Ycf2/FtsHi Complexes as a Major Preprotein Import Route

As shown above, the Ycf2/FtsHi complex is specifically associated with the preprotein translocation process, together with TOC and TIC. To further determine the quantitative contribution of the Ycf2/FtsHi2 complex in this process, we performed an LC-MS/MS analysis of the purified translocation intermediates (Table 1; Supplemental Data Set 1). We chose the pFd (ferredoxin) model preprotein (pFd*-TEV-ProtA; where * denotes the presence of a FLAG tag) for the purification of the translocation intermediates (formed in the presence of 0.1 mM ATP; Table 1, +ATP) because

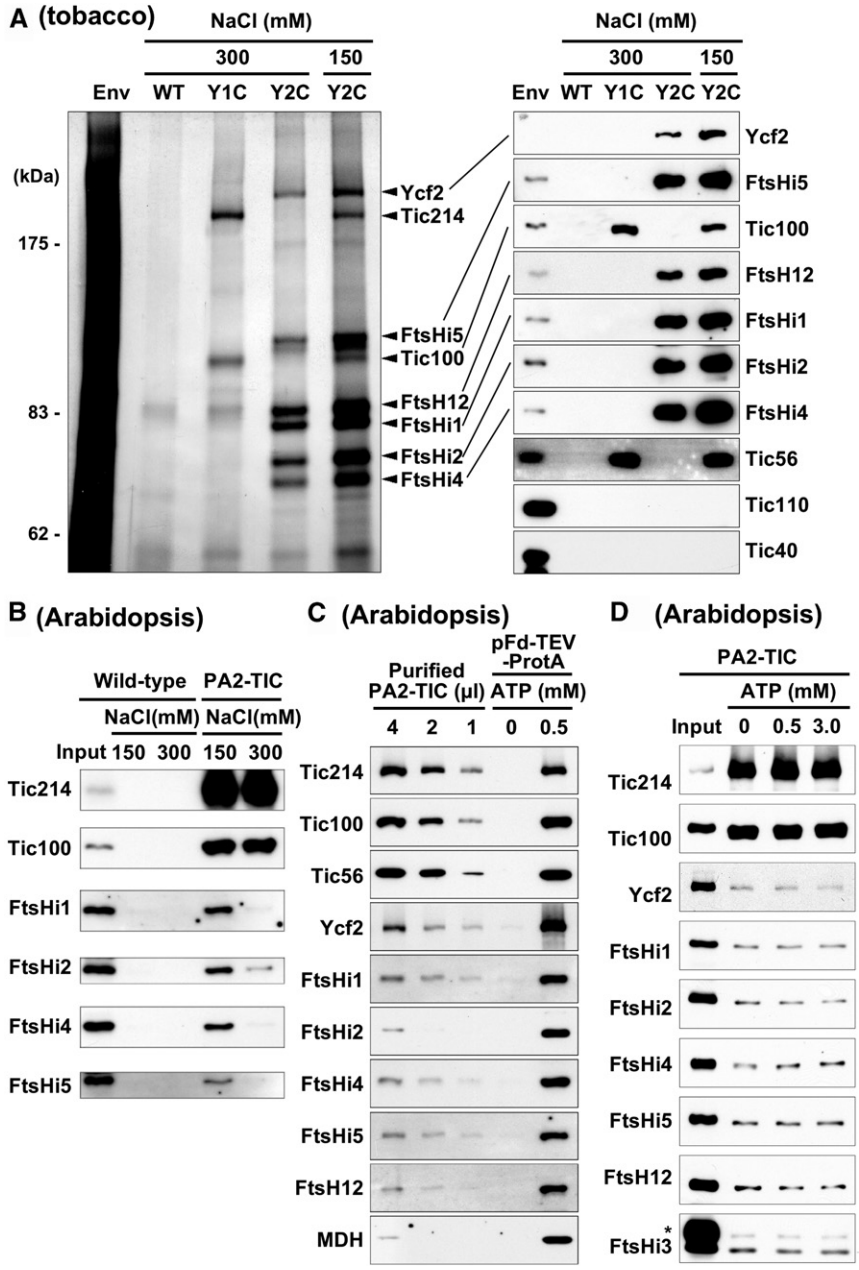

Figure 4. Physical Interaction between the TIC Complex and the Ycf2/FtsHi Complex Observed in Tobacco as well as in Arabidopsis Chloroplasts.

(A) Copurification of the TIC complex with the Ycf2/FtsHi complex from tobacco chloroplasts. Chloroplasts isolated from the Y1C and Y2C transplastomic tobacco lines expressing the HA-tagged forms of Tic214(Ycf1) and Ycf2, respectively, together with those from the parental control wild-type line were solubilized with 1% dodecylmaltoside containing 300 mM NaCl and were separately subjected to purification using anti-HA-agarose beads under the presence of 300 mM NaCl. The similar purification was also performed from Y2C chloroplasts but with the presence of physiological salt concentrations (150 mM NaCl) throughout the solubilization and the purification instead of 300 mM NaCl. The purified fractions eluted from the anti-HA agarose beads by the addition of HA peptides were analyzed by silver staining (left) and by immunoblotting (right). Envelope membranes (Env) isolated from the chloroplasts of the parental wild-type line were also analyzed for reference.

(B) Purification of the Arabidopsis TIC complex from the Protein A-tagged Tic20 (PA2-TIC)-TIC-expressing chloroplasts under the presence of NaCl and association of Ycf2/FtsHi complex components. Chloroplasts isolated from transgenic Arabidopsis plants expressing the Protein A-tagged Tic20 (PA2-TIC) were used for purification of TIC after solubilization of 1% dodecylmaltoside under the presence of 150 or 300 mM NaCl. The wild-type chloroplasts were used as control. The purified proteins were analyzed by SDS-PAGE followed by immunoblotting. Input, 1% of solubilized extracts.

(C) Comparison of amounts of Ycf2/FtsHi complex components associated with the TIC complex with those associated with the translocating preproteins. After in vitro import of pFd-TEV-ProtA in the absence (0 mM) or presence (0.5 mM) of ATP (at 25°C for 10 min) using the wild-type Arabidopsis

of its relatively limited association with the chloroplast envelope in the absence of ATP in our in vitro import experiments (Figure 2B). Two control purifications were conducted: (1) a mock purification from the same amount of chloroplasts or chloroplast membranes without the addition of preproteins (Table 1, Mock); or (2) another purification using the same amount of chloroplasts or chloroplast membranes with preproteins added only after the solubilization with detergent, just prior to purification (Table 1, Post). Except for some known candidates, we excluded nonspecific binders from the list if their ratio of spectrum counts (SPCs) observed in the ATP-dependent translocation intermediates relative to those in either the mock or the post controls (enrichment index) was not greater than 4. We compared two slightly different purification procedures for the translocation intermediates; the intermediates were purified either from digitonin-solubilized whole chloroplast lysates carrying the pFd-TEV-ProtA or from digitonin-solubilized chloroplast membrane extracts carrying the pFd_{FLAG}-TEV-ProtA, using either IgG-Sepharose beads or anti-FLAG-tag monoclonal antibody-conjugated beads, respectively, then eluted by either TEV cleavage or with the FLAG peptide, respectively. In both cases, all the Ycf2/FtsHi complex components were among the proteins with the 20 highest SPCs (Table 1). The receptors and channel proteins of TOC, namely, Toc159, Toc33/Toc34, and Toc75, and the essential TIC components, namely, Tic214 (Ycf1), Tic100, and Tic56, were also all detected in both top-20 lists. Total sum of the SPCs for the TOC, TIC, and Ycf2/FtsHi complex components were comparable in both approaches, strongly indicating their cooperative contribution to the formation of the main translocation pathway across the outer and inner envelope membranes.

Tic20-I, a central component of TIC complex containing Tic214/Tic100/Tic56, was not detected in the MS analysis, but existed stoichiometrically with other TIC constituents and could be easily detected by protein staining following SDS-PAGE (Kikuchi et al., 2013). This is most likely because the Arabidopsis Tic20-I protein is difficult to detect using any kind of MS analysis, as was revealed by the complete absence of its SPC in the AtChloro proteomic database (Table 1, rightmost column) (Ferro et al., 2010).

The Tgd4-like protein (At2g44640), OEP16, and EMB2737 (At5g53860) were commonly found in the Top 20 lists and therefore might be involved in protein translocation; however, this requires further biochemical and genetic study. The Tgd4-like protein, a 44-kD protein, migrated around 60 to 90 kD on the BN-PAGE gel (Supplemental Figure 7C) and therefore is not a firmly attached constituent of TOC, TIC, or the Ycf2/FtsHi complex.

It should be noted that classical Tic proteins (Tic110 and Tic40), a proposed stromal molecular chaperone involved in chloroplast protein import (Hsp90C), and the so-called redox regulators (Tic32, Tic55, and Tic62) had SPCs of almost 0 in one of the LC-MS/MS analyses (Table 1), but had relatively high SPCs in various proteomic analyses reported in the AtChloro database. For other stromal chaperones, namely, Cpn60, Hsp93, and Hsp70, the sensitive LC-MS/MS analyses detected their copurification with translocating preproteins (Table 1). Some of them were also detected in the post and even in the mock control experiments, presumably because of their chaperoning properties, and can therefore be regarded as nonspecific. Using the chloroplast membranes instead of whole chloroplasts diminished most of this nonspecific copurification at a basal level; however, we still observed some SPCs for Hsp93 purified with translocating pFd_{FLAG}-TEV-ProtA.

To clarify the contribution of those stromal molecular chaperones, we purified preprotein-associating proteins following the separation of the membrane and soluble fractions of the chloroplasts (Figure 5A). An in vitro import assay was performed using Arabidopsis chloroplasts with pSSU*-TEV-ProtA in the presence of 0.1 mM ATP for 10 min to accumulate translocation intermediates or in the presence of 3 mM ATP for 30 min to complete translocation. The chloroplasts were then hypotonically ruptured and fractionated into the membrane fraction, containing the envelopes, and the soluble fraction containing the stroma. As shown in Figure 5A (upper panel), the preproteins remained mostly in the membrane fraction after being imported in the presence of 0.1 mM ATP, whereas after incubation with 3 mM ATP for 30 min, a significant amount of mature size (imported) SSU*-TEV-ProtA was observed, mostly in the soluble fraction. These fractions were then used for pull-down experiments using IgG-Sepharose beads to purify preprotein-associating and imported mature protein-associating proteins (Figure 5A, lower panel).

As anticipated, the TIC and Ycf2/FtsHi complex components were associated with translocating preproteins in the membrane fraction in the presence of 0.1 mM ATP, but this association was decreased after a prolonged incubation in the presence of 3 mM ATP (Figure 5A, lower panel). Low levels of Hsp93 and Hsp70 were found to be associated with the imported preprotein in the soluble fraction after import in the presence of 3 mM ATP. Cpn60 also interacted with the translocated protein in the stroma; Cpn60 is involved in the assembly of Rubisco, so the imported SSU (the small subunit of Rubisco) would be expected to interact with Cpn60 in the stroma. We therefore conclude that these stromal chaperones interact with the preproteins (or processed mature proteins) at a rather later stage in the soluble stroma, presumably for folding/assembly. Especially in the case of Hsp93 (ClpC), such an interaction may occur for the quality control (degradation) of incoming

Figure 4. (continued).

chloroplasts, the translocation intermediates were purified under high-salt conditions (250 mM NaCl) and analyzed as shown in Figure 3 (right two lanes). The TIC complex was purified from Arabidopsis plants expressing Protein A-tagged Tic20 (PA2-TIC) under the same conditions (i.e., in the presence of 250 mM NaCl), and purified fractions (4, 2, and 1 μL) were analyzed for comparison. MDH, pdNAD-MDH.

(D) Absence of increased level of association of Ycf2/FtsHi complex components with TIC complex after simple incubation of chloroplasts with ATP without any addition of preproteins. Chloroplasts isolated from the transgenic Arabidopsis plants expressing PA2-TIC were incubated with the indicated amount of ATP (0–3.0 mM) at 25°C for 10 min and subjected for the purification of the PA2-TIC complex as in **(C)** in the presence of 250 mM NaCl. The purified proteins were analyzed by SDS-PAGE and immunoblotting. Input, 1% equivalent of the solubilized extracts of PA2-TIC chloroplasts. Asterisk indicates cross-reactions to abundant thylakoidal Var2, a typical FtsH homolog.

Table 1. Identification of the Translocation Intermediate-Associating Proteins by LC-MS/MS

	Total Spectrum Counts								
	Purified with Translocating pFd-TEV-Protein A from Chloroplasts Using IgG-Sepharose				Purified with Translocating pFd_{FLAG}-TEV-Protein A from Chloroplast Membranes Using αFLAG-Agarose				AtChloro
Identifier	Mock[a]	+ATP	Post[b]	Rank[c]	Mock[a]	+ATP	Post[b]	Rank[c]	Database[d]
TOC components (sum):	(0)	(191)	(25)		(0)	(251)	(3)		
Toc75-III	0	75	13	[2]	0	85	3	[3]	296
Toc159	0	60	5	[4]	0	104	0	[2]	389
Toc34	0	30	3	[8]	0	34	0	[10]	67
Toc33	0	26	4	[9]	0	28	0	[12]	64
TIC components (sum):	(0)	(233)	(7)		(4)	(281)	(6)		
Tic214(Ycf1)	0	157	4	[1]	4	207	6	[1]	317
Tic56	0	45	3	[5]	0	38	0	[6]	64
Tic100	0	31	0	[7]	0	36	0	[8]	51
(Tic20-I)[e]	0	0	0		0	0	0		0
Ycf2/FtsHi components (sum):	(0)	(137)	(7)		(0)	(246)	(0)		
Ycf2	0	33	3	[6]	0	67	0	[4]	50
FtsH12	0	22	0	[10]	0	28	0	[15]	112
FtsHi5	0	20	0	[11]	0	34	0	[11]	36
NAD-MDH	0	17	4	[13]	0	24	0	[14]	313
FtsHi2	0	16	0	[15]	0	35	0	[9]	59
FtsHi4	0	16	0	[16]	0	27	0	[13]	52
FtsHi1	0	13	0	[18]	0	36	0	[7]	78
Other proteins commonly found in the specifically associating Top 20 protein lists of the both experiments									
Tgd4-like (At2g44640)	0	49	0	[3]	0	55	0	[5]	55
OEP16	0	15	0	[17]	0	17	0	[20]	198
EMB2737 (At5g53860)	0	9	0	[20]	0	20	0	[17]	15
Other chaperones									
Hsp93 (-III and -V)	6	29	20		0	17	0		2411
Cpn60α (At2g28000)	10	10	23		0	0	0		1195
Hsp70 (At4g24280)	9	9	17		0	3	0		818
Cpn60β (At1g55490)	8	8	27		0	0	0		1427
Hsp90C (At2g04030)	0	0	0		0	0	0		331
Historical TIC candidate proteins									
Tic110	0	0	12		0	0	0		982
Tic40	0	0	0		0	0	0		215
Tic55	0	0	4		0	3	0		268
Tic62	0	3	11		0	0	0		89
Tic32	0	0	0		0	0	0		12

pFd-TEV-Protein A and pFd_{FLAG}-TEV-Protein A were used for in vitro import experiments with Arabidopsis chloroplasts in the presence of 0.1 mM ATP. Translocation intermediates were purified either from the chloroplasts or from the membrane fraction of the chloroplasts using either the IgG-Sepharose or the αFLAG-agarose and analyzed by LC-MS/MS (+ATP).

[a]Mock-purified samples from the same amounts of chloroplasts or chloroplast membranes without the addition of $pFd_{(FLAG)}$-TEV-Protein A were also analyzed as one negative control (Mock).

[b]Another negative control purification with the excess amount of $pFd_{(FLAG)}$-TEV-Protein A but added only after solubilization of chloroplasts or chloroplast membranes was carried out and analyzed as well (Post).

[c]Only those proteins identified in the Top 20 protein lists (Rank) of the two independent experiments (+ATP) in common with enrichment index above 4 compared to both two different negative controls (Mock and Post) are displayed. All the TOC, TIC, and Ycf2 complex components except Tic20-I were retained in both Top 20 lists.

[d]For reference of their relative easiness/difficulty for MS identification in chloroplasts, total spectrum counts extracted from the AtChloro database (as of March 18, 2018) are shown.

[e]Note that Arabidopsis Tic20-I protein, a central component of TIC, has been known to be an extremely difficult membrane protein to be detected by MS, while this protein could be clearly detected as a translocation intermediate-associating protein by immunoblotting (Kikuchi et al., 2013).

preproteins, as has been proposed recently (Sjögren et al., 2014; Flores-Pérez et al., 2016).

ATP-Dependent Preprotein Handover from TOC-TIC Complexes to the TIC-Ycf2/FtsHi Complex

To dissect the multiple steps involved in preprotein translocation across the envelope membranes in in vitro import experiments, we used a shorter model preprotein, $pSSU_{FLAG}$ (Rubisco small subunit with a FLAG tag; 203 amino acids long), to form early translocation intermediates under low ATP conditions (0.1 mM) for 10 min (Figure 5B, upper panel). Under this condition, $pSSU_{FLAG}$ mostly remained as a preprotein. After the reisolation of the chloroplasts to remove unbound $pSSU_{FLAG}$, a subsequent chase incubation with 3 mM ATP caused the bound preproteins to be imported into the stroma and processed to form a mature

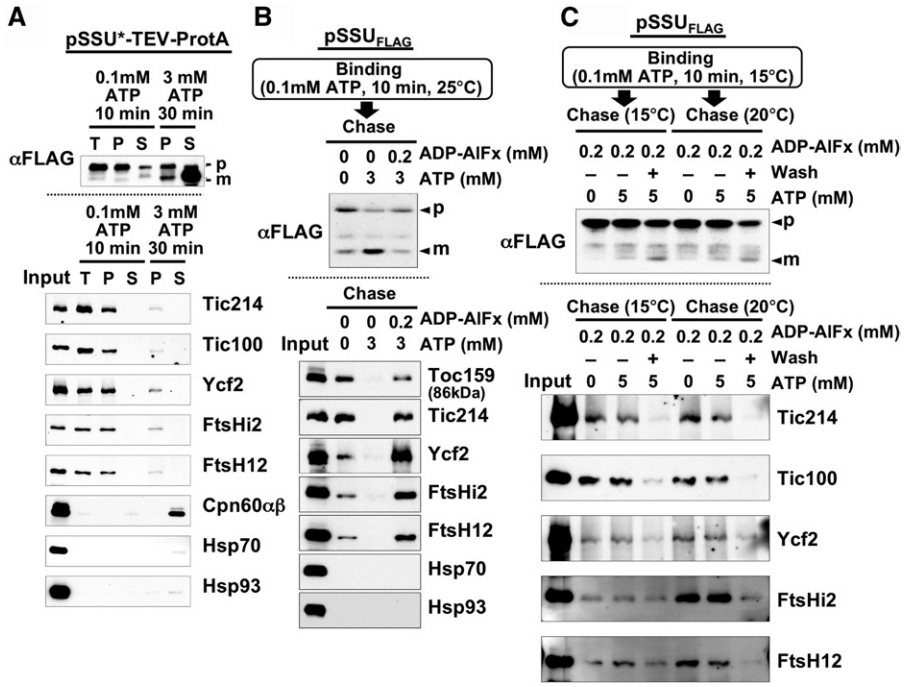

Figure 5. The Ycf2/FtsHi Complex Is Directly Involved in the ATP-Dependent Preprotein Translocation at the Inner Envelope of Chloroplasts.

(A) Association of stromal chaperones occurs at a rather later stage mostly after preprotein translocation into the stroma. In vitro import experiments were performed using Arabidopsis chloroplasts and the purified pSSU*-TEV-ProtA in the presence of 0.1 mM ATP (for 10 min) or 3 mM ATP (for 30 min). After import, chloroplasts (T, total) were ruptured in hypotonic solution (10 mM HEPES-KOH, pH 7.8, and 4 mM $MgCl_2$) and fractionated into the membrane pellets (P) and the soluble supernatants containing stroma (S). Equivalent aliquots of each fraction were analyzed directly by SDS-PAGE followed by immunoblotting with anti-FLAG-tag antibodies (upper panel). p, precursor form; m, mature form. The obtained membrane pellets and supernatant together with total chloroplasts before fractionation (T) were subjected to purification of preprotein-associating proteins as shown in Figure 2. Equivalent amounts of each purified fraction were analyzed by immunoblotting (lower panel). Input, 1% equivalent of digitonin-solubilized total chloroplast extracts used for purification.

(B) The ADP-AlFx causes accumulation of the Ycf2/FtsHi complex-bound form of preproteins. The pSSU$_{FLAG}$ (203 amino acids) synthesized in S30 extracts was incubated with isolated Arabidopsis chloroplasts in the presence of 0.1 mM ATP to accumulate early translocation intermediates (Binding, at 25°C for 10 min). Subsequent chase incubation (at 25°C for 20 min) was performed without any addition or in the presence of 3 mM ATP alone or 3 mM ATP plus 0.2 mM ADP-AlFx. After incubation, aliquots of each reaction were directly analyzed for import of pSSU$_{FLAG}$ by immunoblotting using anti-FLAG-tag antibody (upper panel). p, precursor form; m, mature form. The remainders were subjected to purification of preprotein-associating proteins using anti-FLAG-tag M2 affinity gel instead of IgG-Sepharose beads and analyzed by immunoblotting as in **(A)** (lower panel). Input, 1% equivalent of digitonin-solubilized chloroplast extracts used for purification.

(C) Preproteins arrested as translocation intermediates in the presence of ADP-AlFx can be imported into the chloroplast to form a mature protein by washing out the ADP-AlFx and subsequent addition of excess ATP. After binding in the presence of 0.1 mM ATP (at 15°C for 10 min), translocation intermediates were accumulated in the presence of 0.2 mM ADP-AlFx as in **(B)** but by incubating for 10 min at low temperature (15°C or 20°C) to slow down the translocation process. Complete translocation (formation of mature form) was observed by further chase incubation for additional 20 min in the presence of excess 5 mM ATP only after washing out the ADP-AlFx (Wash). After incubation, aliquots of each reaction were directly analyzed for import of pSSU$_{FLAG}$ as in **(B)** (upper panel). The remainder was subjected to purification of preprotein-associating proteins using anti-FLAG-tag M2 affinity gel and analyzed as in **(B)** (lower panel).

protein. If ADP-AlFx, an ATP-hydrolysis transition-state analog, was included during the chase incubation in addition to 3 mM ATP, this import was completely blocked, indicating that ATP hydrolysis is required during this translocation step.

We next purified the preprotein (or mature protein)-interacting proteins/complexes from the chloroplasts after these different import reactions using anti-FLAG-tag monoclonal antibody-conjugated Sepharose beads (Figure 5B, lower panel). After an initial incubation with 0.1 mM ATP, Toc159 and Tic214 were predominantly purified with the preproteins, indicating that bound pSSU$_{FLAG}$ largely remained in the TOC- and/or TIC-bound states. This interaction disappeared when the bound preproteins were completely imported into the stroma after the chase incubation in the presence of 3 mM ATP. By contrast, if ADP-AlFx was present during the chase incubation, the association of the Ycf2/FtsHi complex components with the preproteins became remarkable, while the interactions with Toc159 and Tic214 were decreased. These results indicate that inhibiting the ATP hydrolysis required for translocation into the stroma caused a marked accumulation of Ycf2/FtsHi complex-bound preproteins concomitant with the

significant preprotein release from TOC and/or TIC. We did not observe any accumulation of Hsp93- or Hsp70-bound preproteins under these experimental conditions.

To confirm that the Ycf2/FtsHi complex-bound preproteins that accumulated in the presence of ADP-AlFx could be imported after the removal of ADP-AlFx with the addition of excess ATP, we performed another set of import experiments (Figure 5C). Binding and chase experiments were performed as described above, but at lower temperatures (15°C or 20°C) to slow down the import reactions. In the chase incubation, the bound preproteins formed in the presence of 0.1 mM ATP could not be imported into the chloroplasts to form mature proteins if ADP-AlFx was present, even if treated with excess (5 mM) ATP Figure 5C, upper panel). If the added ADP-AlFx was subsequently removed from the chloroplasts, we observed low but significant amounts of processed mature and thus imported proteins during the chase incubation with 5 mM ATP. As shown in the lower panel of Figure 5C, the accumulated preproteins could be released from the Ycf2/FtsHi complex-bound state to complete the translocation during the chase incubation with excess ATP only after removal of ADP-AlFx. These data indicate that the Ycf2/FtsHi complex-bound state is the ATP-hydrolysis-requiring step for subsequent preprotein translocation across the inner envelope membrane.

Translocating Preprotein Transit Peptides Directly Interact with Ycf2/FtsHi Complex Components

We next explored whether the Ycf2/FtsHi complex components directly recognize a transit peptide moiety on the preproteins during the translocation process. We constructed another set of preproteins, as shown in Figure 6A. All of the Cys residues in the original HA-tagged pFd (ferredoxin) preprotein were substituted with Ser residues [pFdvari-HA(ΔC)], then a unique Cys residue was introduced into the 6th or 9th position of the transit peptide to generate pFdvari-HA(6C) or pFdvari(9C), respectively. These substitutions did not cause any change in their import abilities. As summarized in Figure 6B, *Escherichia coli*-expressed purified preproteins were used in in vitro import experiments performed in the absence (0 mM) or presence (0.5 mM) of ATP for 20 min at 25°C. The chloroplasts were reisolated and treated with bismaleimidohexane (BMH), a membrane-permeable cross-linker for covalent, irreversible conjugation between two sulfhydryl groups. The chloroplasts were then completely solubilized and denatured using SDS. After trapping the SDS with excess Triton X-100, the cross-linked adducts containing the preproteins were analyzed in reciprocal coimmunoprecipitation experiments (co-IP); immunoprecipitation with antibodies against the Ycf2/FtsHi complex components followed by immunodetection with anti-HA-tag antibodies (Figure 6C) or immunoprecipitation with anti-HA-tag antibodies followed by immunodetection with antibodies against the Ycf2/FtsHi complex components (Figure 6D).

After the 20-min import reaction in the presence of 0.5 mM ATP, very strong cross-linked products were observed at around the 135-kD position (Figure 6C, center panel, input), which were immunoprecipitated with anti-FtsHi1 antibodies. The occurrence of the cross-linked bands was completely dependent on the presence of the unique Cys residues in the transit peptide of preprotein and on the presence of ATP during the import reactions. The Cys at position 6 gave stronger cross-linked bands than that at position 9. The observed 135-kD size was slightly larger than the sum of the apparent molecular sizes of FtsHi1 and pFdvari-HA on the SDS-PAGE gel, which were 83 and 23 kD, respectively, presumably due to the branched structure of the cross-linked adduct. Very similar cross-linked proteins were observed when the immunoprecipitation was performed with anti-HA-tag antibodies followed by immunodetection with the anti-FtsHi1 antibodies (Figure 6D, left panel). These results indicate that FtsHi1 was predominantly cross-linked with the transit peptide moiety of the preproteins at an apparent 1:1 ratio after 20-min import reactions in the presence of 0.5 mM ATP.

When this import was blocked in the middle of an incubation (after 10 min) by adding 0.2 mM ADP-AlFx, the cross-linked profiles were significantly altered. Cross-linking between FtsHi5 and Cys at position 9 of the preprotein observed at around 180 kD became more prominent (Figures 6C and 6D, right panels) concomitantly with the decrease of cross-linked FtsHi1 products. The apparent molecular size of FtsHi5 on the SDS-PAGE gel is ~130 kD, suggesting that the observed 180-kD band likely corresponds to the 1:1 cross-linked product with the preprotein. These observations suggest the intersubunit movement of the transit peptide of the preprotein through the Ycf2/FtsHi complex during the ATP-dependent translocation, as has previously been widely proposed to take place through the AAA-ATPase hexameric ring structure (Gates et al., 2017; Puchades et al., 2017).

We performed similar cross-linking experiments to clarify any direct interaction between Ycf2 and the translocating preproteins (Supplemental Figure 8). Cross-linked products were commonly observed at fairly high molecular mass regions of the SDS-PAGE gel using a reciprocal co-IP analysis with anti-HA-tag antibodies and anti-Ycf2 antibodies (Supplemental Figures 8A and 8B). Formation of the Ycf2-preprotein cross-linked products were completely ATP dependent in the import reactions and Cys-dependent in the transit peptide of the preprotein, indicating that Ycf2 also directly interacts with transit peptide moieties on the translocating preproteins.

Ycf2/FtsHi Complex Components Are Essential in Arabidopsis, While the FtsH12 Conserved Zinc Binding Motif Is Dispensable

Ycf2 is essential in tobacco (Drescher et al., 2000) and the green algae Chlamydomonas (Nickelsen, 2005); moreover, individual knockout mutations of the Ycf2/FtsHi complex components in Arabidopsis, namely, FtsHi1 (*ftshi1-2*) (Kadirjan-Kalbach et al., 2012), FtsHi2 (*emb2083*), FtsHi4 (*emb3144*), and FtsHi5 (*emb2458*), as well as FtsH12 (*emb1047-1*), are embryo lethal (Meinke, 2013; Lu et al., 2014). As mentioned before, among the Ycf2/FtsHi complex components, only FtsH12 possesses a zinc binding motif (Figure 1A). We therefore determined whether this zinc binding motif is necessary for the essential function of FtsH12 using a complementation analysis (Figure 7). Since the homozygous *ftsh12* knockout (*emb1047-1*) is embryo lethal, a heterozygous line containing this mutation was transformed with either the wild-type *FTSH12* cDNA or the mutant *FTSH12(H769Y)* cDNA placed under control of the 35S promoter

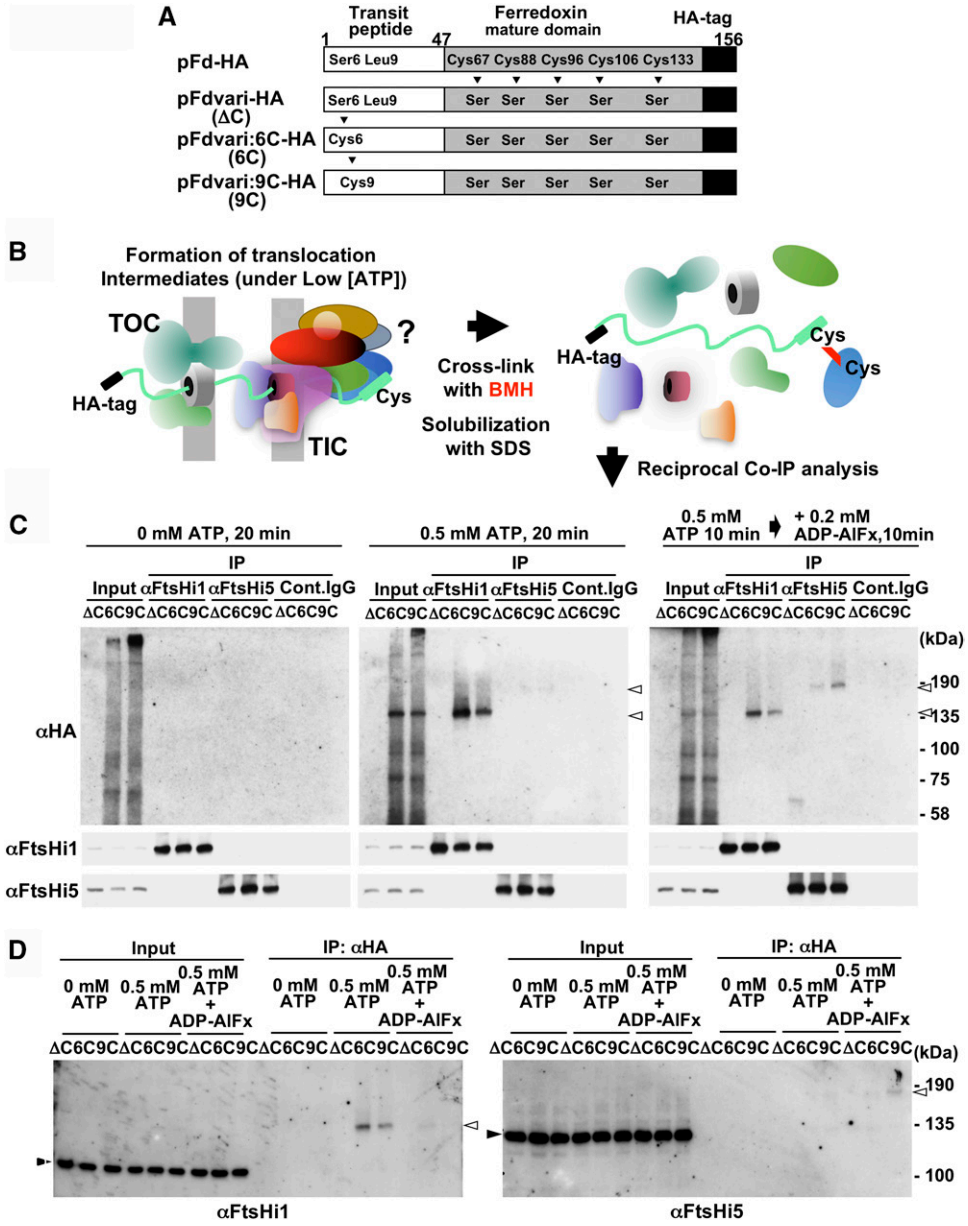

Figure 6. Direct Interaction between the Transit Peptide Moiety of Translocating Preproteins and the Ycf2/FtsHi Complex Components Revealed by Site-Specific Chemical Cross-Linking.

(A) Schematic presentations of the model preproteins used for site-specific cross-linking. All Cys residues in pFd-HA, a HA-tagged ferredoxin preprotein (156 amino acids), were substituted by Ser residues to construct pFdvari-HA(ΔC). Then, Ser-6 and Leu-9 residues were individually mutated to Cys and resulting constructs were named pFdvari-HA(6C) and pFdvari-HA(9C), respectively.

(B) Procedures of chemical cross-linking. Translocation intermediates were accumulated under low ATP conditions and the reisolated chloroplasts were subjected to chemical cross-linking with the membrane-permeable cross-linker BMH, which covalently cross-links sulfuhydryl groups of two adjacent Cys residues. After complete solubilization and denaturation by addition of 1% SDS, immunoprecipitation was performed using the anti-HA agarose or using the purified IgGs specific to the Ycf2/FtsHi complex components that had been conjugated to Protein A Sepharose. Immunoprecipitated proteins were analyzed for coimmunoprecipitation of directly interacting proteins (Reciprocal Co-IP) by SDS-PAGE followed by immunoblotting.

(C) Arabidopsis chloroplasts were incubated with pFd-HA derivatives, ΔC, 6C, and 9C, separately in the absence (0 mM) (left panels) or presence (0.5 mM) (central panels) of ATP at 25°C for 20min. For experiments shown in the right panels, import reactions were performed in the presence of 0.5 mM ATP at 25°C for 10 min followed by further 10 min incubation at 25°C after addition of 0.2 mM ADP-AlFx. After import reactions, cross-linking with BMH and subsequent SDS-solubilization/denaturation were performed as described above. Immunoprecipitation (IP) was performed using either the purified anti-FtsHi1(αFtsHi1), anti-FtsHi5(αFtsHi5), or control rabbit IgGs (Cont.IgG). Immunoprecipitates were analyzed by SDS-PAGE followed by immunoblotting using anti-HA-tag antibody(αHA) to detect cross-linked and coimmunoprecipitated pFdvari-HA derivatives (white arrowheads, top

(Figure 7A). Similar His-to-Tyr substitutions in the first His residue of the conserved HEXXH zinc binding motif have been demonstrated to abolish the protease activities of FtsH as well as other zinc metalloenzymes (Laustsen et al., 2001; Saikawa et al., 2002). The T2 offspring carrying the transgene were analyzed for the presence or absence of the wild-type *FTSH12* gene at the *FTSH12* genomic locus. For both transgenes, *FTSH12(wild-type)* and *FTSH12(H769Y)*, we were able to obtain homozygous T-DNA knockout lines (*ftsh12*/–) carrying either transgene, which exhibited normal wild-type growth (Figure 7B) and levels of FtsH12 protein comparable to the wild type (Figure 7C). The complete absence of the authentic wild-type allele was confirmed using genomic PCR (Figure 7D) and the subsequent direct DNA sequencing of the PCR-amplified fragments (Figure 7E). Chloroplasts isolated from these lines showed indistinguishable preprotein import abilities, as shown in Figures 7F and 7G. We therefore concluded that, although FtsH12 retains the zinc binding motif, the motif is dispensable for its essential function.

In Vitro Import Defects Observed in the *arc1* Mutant Carrying a Single Amino Acid Substitution in FtsHi1

While the complete knockout of the *FtsHi1* gene (*ftshi1-2*) is lethal, the *arc1* (*ftshi1-1*) mutation is not. This mutant, which carries a point mutation (S524F) near the Walker B motif and exhibits a slightly pale phenotype, was initially identified as a chloroplast-division mutant (Kadirjan-Kalbach et al., 2012) (Figure 8A). However, the detailed analyses performed by these researchers led them to conclude that FtsHi1 does not function directly in division. Isolated *arc1* chloroplasts contain a comparable level of FtsHi1 protein to those of the wild type (Figure 8B) and form assembled Ycf2/FtsHi complexes (Figure 8C); however, they have marked in vitro protein import defects (Figure 8D). Binding (at low ATP) and chase (with high ATP) experiments confirmed that this impairment occurred at the high ATP-requiring translocation step at the inner envelope after the initial binding to TOC, as revealed by the inefficient accumulation of imported mature proteins after the chase incubation (Figure 8E). The impairment in protein import was more clearly observed when purified preproteins were used as substrates instead of using those synthesized in cell-free in vitro translation systems (Figure 8F). Figure 8G depicts a quantitative comparison of import efficiencies for the same preprotein, pFd*-TEV-ProtA, synthesized in the cell-free translation system or purified from *E. coli* cells, confirming that more drastic import defects were observed for the purified preproteins.

We confirmed that the observed import defects could be complemented with the wild-type *FTSHi1* transgene (Figure 8G, *arc1 comp4*). The accumulated preproteins in the *arc1* mutant remained associated with the membrane but were not imported into the stroma (Figure 8H). In general, preproteins synthesized in the cell-free translation systems tended to be maintained in import-competent unfolded conformations because of the presence of the various molecular chaperones included in these translation systems. The purified preproteins used in the import experiments had been urea-denatured before import, but after their addition into the import reaction mixtures containing chloroplasts, their folding should presumably proceed very rapidly. This is the most likely reason why the preproteins synthesized in the cell-free translation systems showed less impairment during import than the purified preproteins and also why the *arc1* mutant exhibited a pale phenotype but remained viable because, in vivo, there should be various chaperone proteins in the cytosol that can maintain import-competent conformations of newly synthesized preproteins. The observed in vitro import defects in the *arc1* mutant are consistent with the idea that the FtsHi1-containing Ycf2/FtsHi complex provides a pulling force during the preprotein translocation across the inner envelope membrane, functioning as a trans-side ATP-driven import motor (Figure 1B).

ATP Binding to the AAA-ATPase Domain of FtsHi1

Although the FtsHi proteins possess domains that show high sequence similarity to the AAA-ATPase domain of FtsH and retain key amino acid residues in the Walker ATPase A and B motifs, their ATP binding and ATP hydrolysis abilities have not been investigated. Since the *arc1* mutant contains a substitution mutation of an amino acid residue near the Walker B motif in FtsHi1 and exhibits remarkable protein import defects, we conducted experiments to assess the ATP binding/hydrolysis ability of recombinant FtsHi1 and investigate the effect of the *arc1* mutation on these functions. To this end, we first expressed the entire C-terminal domain of Arabidopsis FtsHi1 in *E. coli* cells as a recombinant protein; however, the expressed proteins were recovered exclusively in inclusion bodies even when expressed at low temperatures as a fusion protein with a large soluble protein GST (GST-FtsHi1C_L) (Figures 9A and 9B). This is presumably because, in vivo, FtsHi1 forms a hetero-oligomer with other components of the Ycf2/FtsHi complex, meaning the solely expressed FtsHi1 C-terminal domain cannot be folded properly or be present in a soluble form.

Next, we expressed a shorter fragment of the C-terminal domain of FtsHi1, containing only the AAA-ATPase domain, as a GST fusion protein (GST-FtsHi1C_S), which was able to be recovered in a soluble form (Figures 9A to 9C). Unexpectedly, the purified GST-FtsHi1C_S showed no ATPase activity even in the presence of equimolar amounts of preproteins, most likely because

Figure 6. (continued).

panels). Specificities of immunoprecipitations were confirmed by immunoblotting using anti-FtsHi1 (middle panels) or anti-FtsHi5 antibodies (bottom panels). Input, 1% equivalent of digitonin-solubilized total chloroplast extracts used for purification.

(D) As in **(C)**, but anti-HA-tag(αHA) agarose was used for immunoprecipitation and the cross-linked and coimmunoprecipitated FtsHi1 (left panel) and FtsHi5 (right panel, arrowheads) were detected by immunoblotting. Note that apparent sizes of ATP-dependent cross-linked products observed in the reciprocal co-IP analysis shown in **(C)** and **(D)** were perfectly matched with each other and well correspond to the estimated size of 1:1 cross-linked product between a pFdvari-HA and FtsHi1 or FtsHi5 proteins.

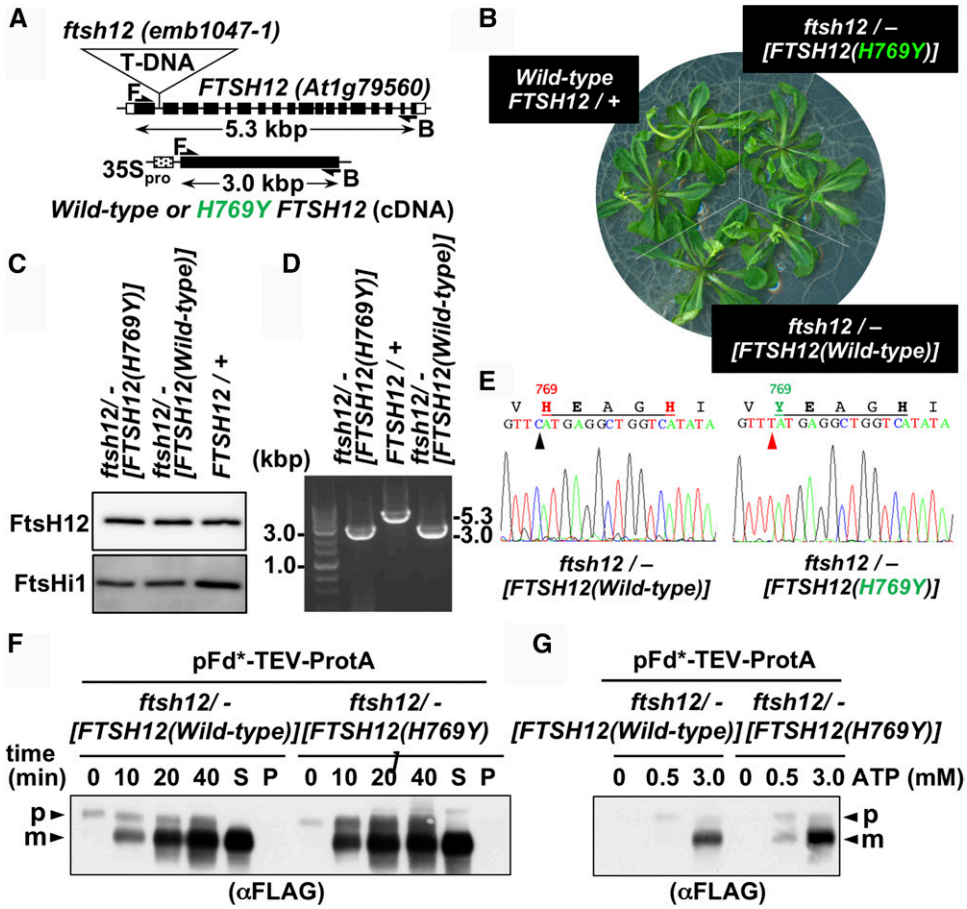

Figure 7. A Remaining Zinc Binding Motif of FtsH12 Is Dispensable for the Essential Function of FtsH12 in Arabidopsis.

(A) The position of T-DNA insertion in the *FTSH12* locus on the Arabidopsis genome. Transgene cDNA constructs placed under the 35S promoter ($35S_{pro}$) together with the positions of PCR primers used for genotyping were also depicted.

(B) Functional complementation of the embryo-lethal homozygous *ftsH12* null mutant (*emb1047-1*) by expressing the FtsH12(H769Y) mutant. Individuals carrying the indicated genotypes were grown on the MS media containing 2% sucrose for 25 d.

(C) Protein levels in the transformants and in the wild type were analyzed by SDS-PAGE and immunoblotting. Ten micrograms of total protein extracts of each seedling was analyzed.

(D) PCR genotyping confirmed the homozygous T-DNA insertions in the *ftsh12* locus of the obtained transformants. The forward (F) and backward (B) primers shown in **(A)** were used.

(E) The genomic PCR fragments obtained from the transformants were directly sequenced. Only the mutated region was shown.

(F) The FtsH12(H769Y) mutant showed normal chloroplast protein import. Chloroplasts were isolated from the homozygous T-DNA inserted line expressing the wild-type FtsH12 or the mutant FtsH12(H769Y) and used for the in vitro import experiments with pFd*-TEV-ProtA as a model preprotein. Import was performed in the presence of 3 mM ATP for 0, 10, 20, and 40 min and analyzed by SDS-PAGE followed by immunoblotting using anti-FLAG antibody. After 40 min incubation, another aliquot of chloroplasts was ruptured to separate the soluble supernatant containing stroma (S) from the membrane pellet (P) and analyzed similarly. m, mature form; p, precursor form.

(G) ATP-dependent import of pFd*-TEV-ProtA into the chloroplasts expressing the wild-type FtsH12 or FtsH12(H769Y) mutant was analyzed as in **(F)**.

the solely expressed FtsHi1 AAA domain cannot properly form the substrate binding structure required for efficient ATP hydrolyzing activity. Despite this, it exhibited high ATP binding ability, as shown in Figure 9D. We used trinitrophenyl-ATP (TNP-ATP), a fluorescent ATP analog, for the ATP binding assay (LaConte et al., 2017). When excited at 410 nm, TNP-ATP showed a fluorescence peak at around 550 nm. Upon the binding of TNP-ATP to the protein leading the TNP group into a more hydrophobic environment, increased fluorescence and a blue shift of the emission maximum to 540 nm were observed. In comparison with the basal level of fluorescence change for GST with a peak around 550 nm, which indicates nonspecific binding, GST-FtsHi1C_S exhibited a saturable binding of TNP-ATP with an increased peak at 540 nm (Figure 9D). The observed binding affinity of TNP-ATP to GST-FtsHi1C_S was relatively high (K_d < 2 μM) (Figure 9E).

To confirm the specificity of this binding of TNP-ATP to the anticipated ATP binding pocket of the FtsHi1C_S, we explored

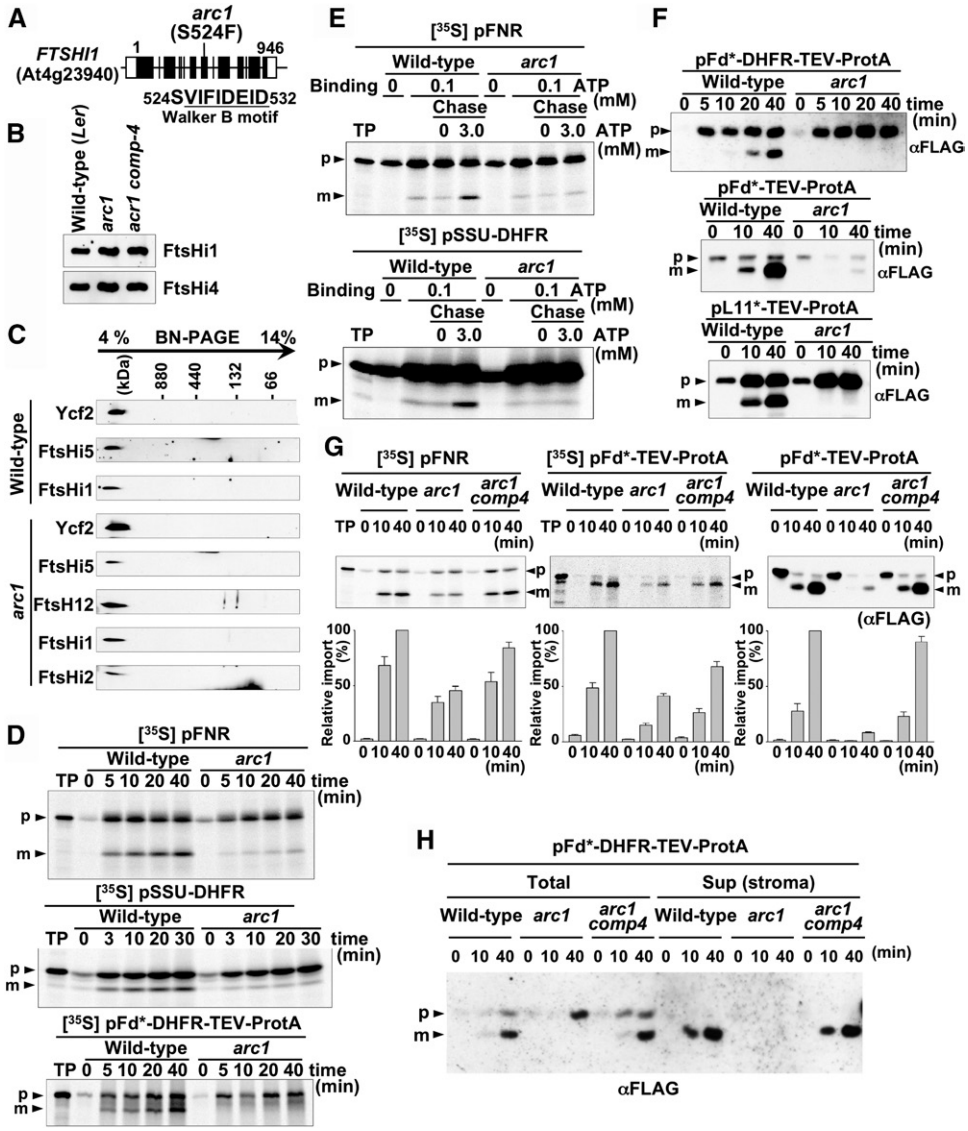

Figure 8. The *arc1* Mutation (S524F) Near the Walker B Motif of FtsHi1 Causes Severe Protein Import Defects.

(A) The position of *arc1* mutation in the *FTSHi1* locus on the Arabidopsis genome. The *arc1* encodes a mutant form of FtsHi1 whose Ser-524 was substituted with Phe.

(B) The protein expression levels in the *arc1* mutant were compared with those in the wild type by SDS-PAGE followed by immunoblotting. Forty micrograms of proteins of total cell extracts was loaded. The wild-type genomic copy of *FTSHi1*-complemented chloroplasts (*arc1 comp4*) was also analyzed.

(C) The *arc1* (*ftsHi1-1*) mutation does not affect the formation of the Ycf2/FtsHi complex. Chloroplasts (20 μg chlorophyll) isolated either from the wild-type or the *arc1* seedlings were subjected to 2D-BN/SDS-PAGE analysis followed by the immunoblotting after solubilization with 1% Triton X-100 in the presence of 300 mM NaCl as shown in Figure 3A.

(D) The *arc1* chloroplasts impair the ATP-dependent in vitro import of various preproteins. In vitro import experiments were performed in the presence of 3 mM ATP using chloroplasts (50 μg chlorophyll) isolated either from the wild-type or the *arc1* seedlings. Import time-course analysis with [^{35}S]-labeled preproteins synthesized in the cell-free lysates is shown. Chloroplasts isolated from the import reactions after the indicated time of incubation at 25°C were analyzed by SDS-PAGE followed by autoradiography to detect [^{35}S]-labeled proteins. p, precursor form; m, mature form. TP, 10% of translated preproteins used for the import reaction.

(E) The import defects of the *arc1* mutant occur at the high ATP-requiring preprotein translocation step across the inner membrane rather than the initial binding step. In vitro import experiments were performed as in **(D)** but initially without (0 mM) or with 0.1 mM ATP for 10 min at 25°C to form early translocation intermediates (Binding). After reisolation of chloroplasts from each reaction, chase incubations were performed in the absence (0 mM) or the presence (3 mM) of ATP for 40 min at 25°C and analyzed as in **(D)**.

(F) Import time-course analysis with the *E. coli*-expressed purified preproteins, pFd*-DHFR-TEV-ProtA, pFd*-TEV-ProtA, and pL11*-TEV-ProtA, were performed as in **(D)**. Urea-denatured purified preproteins (1–2 μg) were incubated with chloroplasts (50 μg chlorophyll) isolated either from the wild-type

whether ATP could displace prebound TNP-ATP from the FtsHi1C_S. As shown in Figure 9F, after the formation of the GST-FtsHi1C_S:TNP-ATP complex, the addition of excess ATP led to a reduction in fluorescence at 540 nm in a ATP concentration-dependent manner, indicating the displacement of bound TNP-ATP with ATP. Using this assay system, we intended to investigate the influence of the *arc1* mutation, namely, Ser-524 to Phe-524, on the ability of FtsHi1 to bind ATP; however, GST-FtsHi1C_S(S524F) was exclusively formed in inclusion bodies in *E. coli* (Figure 9G). Moreover, several trials for the refolding of urea-denatured GST-FtsHi1C_S(S524F) were unsuccessful; therefore, we were unable to assess the ATP binding ability of this protein. While the effect of the *arc1* mutation on the function of FtsHi1 should be investigated in more detail using other methods in the future, one may conclude that the single Ser-to-Phe mutation at position 524 of FtsHi1 has a significant structural consequence in the folding of this AAA-ATPase domain, which likely cause the observed protein import defects.

Decreasing pdNAD-MDH Does Not Significantly Affect the Formation of the Ycf2/FtsHi Complex but Conditionally Impairs Preprotein Import

As shown above, the Ycf2/FtsHi complexes in Arabidopsis and tobacco possess MDH (pdNAD-MDH) as an embedded constituent. While pdNAD-MDH in Arabidopsis is indispensable for plant viability (Beeler et al., 2014), the decreased levels of pdNAD-MDH in *miR-mdh-1* chloroplasts (Supplemental Figure 9A) did not significantly affect the integrity of the 2-MD Ycf2/FtsHi complex (Supplemental Figure 9B) or the preprotein import efficiency in vitro when exogenous ATP was supplied (Supplemental Figure 9C). pdNAD-MDH is proposed to contribute to the ATP supply of heterotrophic/nonphotosynthetic plastids and chloroplasts in darkness by regenerating NAD+ from NADH for continuous triose phosphate oxidation and ATP production (Beeler et al., 2014). Indeed, preproteins were efficiently translocated into wild-type chloroplasts in the dark even without the addition of ATP in the presence of dihydroxyacetone phosphate (DHAP) and oxaloacetate (OAA), the latter of which is a substrate for pdNAD-MDH (Supplemental Figure 9C). This DHAP/OAA-driven import was significantly impaired in the *miR-mdh-1* chloroplasts; however, this does not necessarily mean that pdNAD-MDH in the Ycf2/FtsHi complex rather than stromally localized pdNAD-MDH serves this DHAP/OAA-driven import. It remains to be determined whether the Ycf2/FtsHi complex-incorporated pdNAD-MDH is responsible for this import and also for its indispensability.

Inhibition of Chloroplast Translation by Spectinomycin Causes Deficiency in Chloroplast-Encoded Tic214(Ycf1) and Ycf2 Accumulation and Abolishes Growth of Arabidopsis Seedlings

FtsHi3 was found to be associated to a certain extent with some translocating preproteins (Supplemental Figure 3); however, the homozygous knockout mutant *fsthi3* in Arabidopsis was viable and did not show any significant growth defects or in vitro preprotein import defects (Supplemental Figure 10). FtsHi3 likely forms a 1-MD complex distinct from the essential 2-MD Ycf2/FtsHi complex (Figure 3A), suggesting that FtsHi3 has a redundant function. FtsHi3 is not present in the 1-MD TIC complex (Kikuchi et al., 2013); therefore, whether FstHi3 associates with any other partner proteins is yet to be determined (Figure 1B).

As shown above, Tic214(Ycf1) and Ycf2 are essential components of TIC and the Ycf2/FtsHi complex, respectively, and are encoded by the chloroplast genome. Spectinomycin is known to inhibit translation in the chloroplasts; growing Arabidopsis plants on spectinomycin-containing media results in albino seedlings that cease growth at a very early stage (Parker et al., 2016). We analyzed protein accumulation in Arabidopsis albino seedlings grown on spectinomycin-containing media (Figure 10). As reported, the wild-type seedlings exhibited severe growth retardation with an albino phenotype and ceased to grow after 35 d even when glucose was included in the media (Figure 10A). No accumulation of Ycf2 or Tic214(Ycf1) was observed in the albino seedlings (Figures 10B and 10C), confirming that chloroplast translation including production of Tic214(Ycf1) and Ycf2 is both required for photosynthetic growth and crucial for Arabidopsis viability.

Tic214(Ycf1) forms the TIC complex with Tic100, Tic56, and Tic20-I in photosynthetic chloroplasts (Kikuchi et al., 2013; Nakai, 2018). On the spectinomycin media, the protein levels of Tic100 and Tic56 were largely reduced and no Tic20-I accumulation was observed (Figure 10C). Some housekeeping plastid proteins such as cpHsp70 were still present to a certain extent. In contrast, remarkably elevated levels of Tic20-IV, a nonessential minor isoform

Figure 8. (continued).

or from the *arc1* mutant seedlings in the presence of 3 mM ATP at 25°C. At indicated time points, chloroplasts were reisolated, washed, and analyzed by SDS-PAGE followed by immunoblotting using anti-FLAG tag antibody.

(G) Comparison of import of the purified preproteins with that of [^{35}S]-labeled preproteins synthesized in the cell-free lysates. Import experiments were performed with the [^{35}S]-labeled pFNR (left) or pFd*-TEV-protA (center) synthesized in the cell-free lysates or with the purified pFd*-TEV-ProtA (right) and analyzed by autoradiography or immunoblotting as in **(D)** and **(F)**, respectively. The wild-type *FTSHi1*-complemented chloroplasts (*arc1 comp4*) (Kadirjan-Kalbach et al., 2012) were also analyzed as controls. Processed mature proteins (M) were quantified as described in Methods and are indicated by bar graphs at the bottom (n = 3). The amount of mature proteins observed after 40 min import with the wild-type chloroplasts was set to 100%.

(H) Precursor form accumulated after import reactions in the *arc1* chloroplasts remained membrane-bound. Import time-course analysis with the purified preproteins, pFd*-DHFR-TEV-ProtA, was performed as in **(F)**. After import, chloroplasts (Total) were ruptured in hypotonic solution (10 mM HEPES-KOH, pH 7.8, and 4 mM $MgCl_2$) and the soluble supernatants containing stroma (Sup) were obtained by centrifugation to remove membrane pellets and membrane-bound preproteins. Equivalent amounts of the total and Sup fractions were analyzed by SDS-PAGE followed by immunoblotting using anti-FLAG-tag antibody.

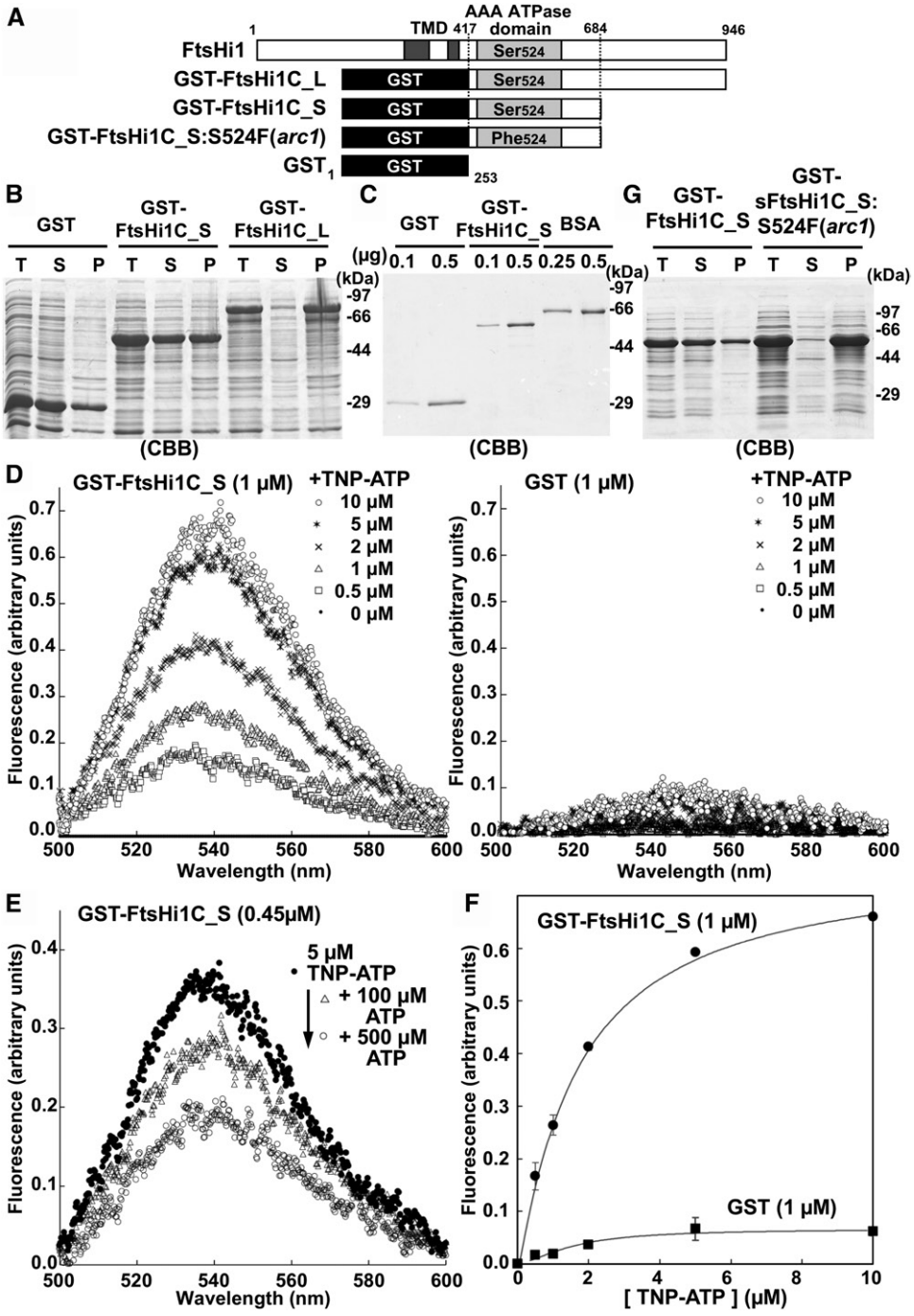

Figure 9. Analysis of ATP Binding to FtsHi1.

(A) Schematic representation of domain structure of Arabidopsis FtsHi1 and the GST-fusion proteins used for the analysis of ATP binding. The corresponding fusion genes were cloned into a pCold-GST vector. GST, glutathione *S*-transferase (from *Schistosoma japonicum*); TMD, transmembrane domain. FtsHi1C_L and FtsHi1C_S are long and short form of the C-terminal domain of FtsHi1.

(B) GST, GST-FtsHiC_L, and GST-FtsHiC_S were expressed in *E. coli* cells at 15°C. Cells were suspended in 50 mM Tris-HCl, pH 7.5, and 150 mM NaCl and disrupted by freeze-thaw cycles with bath sonication and separated into soluble (S) and insoluble pellet (P) fractions. Equivalent amounts of each fraction and total cell extracts (T) were analyzed by SDS-PAGE followed by Coomassie blue staining.

(C) Purified GST and GST-FtsHi1C proteins were analyzed by as in **(B)** with BSA for comparison.

(D) TNP-ATP binding assay of the purified GST-FtsHiC_S (left panel) and the GST (right panel). Fluorescence emission spectra (excitation 410 nm) of TNP-ATP bound to the purified proteins (1 μM). Reference spectra obtained with the corresponding concentration of TNP-ATP without any addition of protein and those with 1 μM proteins but no added TNP-ATP were subtracted as background.

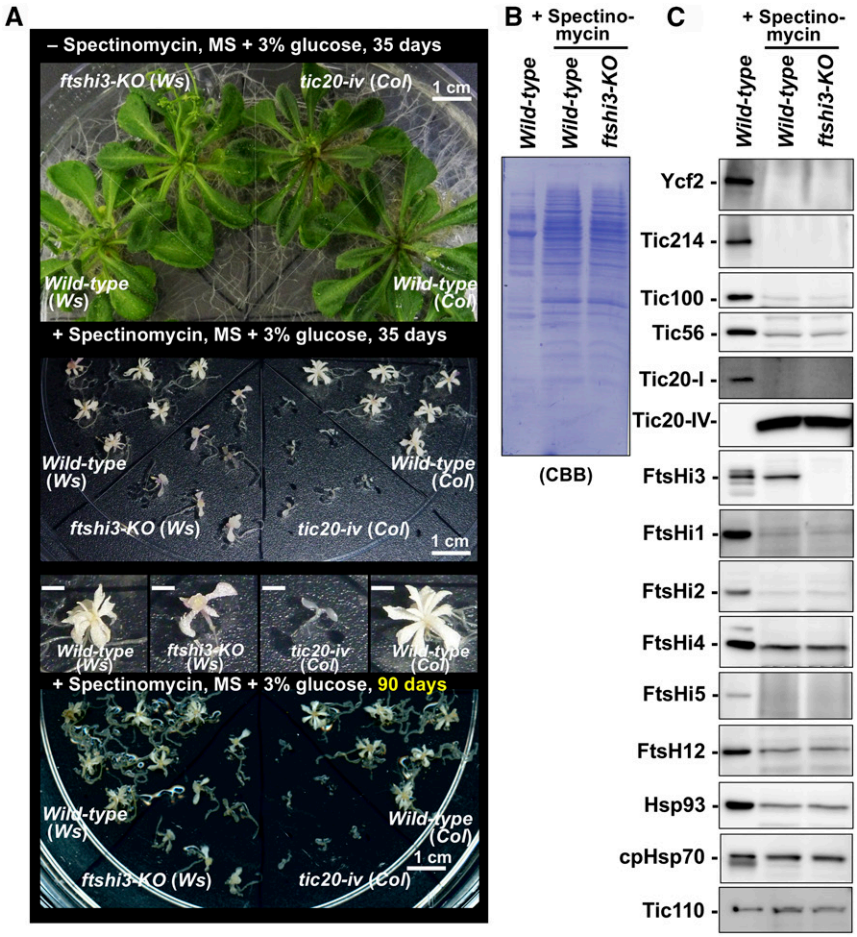

Figure 10. Inhibition of Chloroplast Translation by Spectinomycin Causes Deficiency in Chloroplast-Encoded Tic214(Ycf1) and Ycf2 Accumulation and Abolishes Growth of Arabidopsis Seedlings.

(A) Homozygous knockout mutants for FtsHi3 (*ftsHi3-KO*) or Tic20-IV (*tic20-iv*), a minor isoform of Tic20, were grown on MS media for 35 d with (middle) or without (top) 50 μg/mL spectinomycin together with corresponding wild types (Parker et al., 2016). No further growth on spectinomycin-containing media from 35 d after sowing onward (90 d, at the bottom).

(B) and **(C)** Proteins extracted from the 35-d-old seedlings of wild-type and *ftshi3-KO* mutant were analyzed by Coomassie Brilliant Blue (CBB) staining **(B)** and immunoblotting **(C)**. Five micrograms of total proteins of the wild-type seedlings grown in the absence of spectinomycin and 20 μg of total proteins of the wild-type or the *ftshi3-KO* seedlings grown in the presence of spectinomycin were loaded. Remarkably high expression of Tic20-IV was observed in the seedlings grown in the presence of spectinomycin.

of Tic20, were observed (Figure 10C). This elevated Tic20-IV was absolutely required for the residual albino growth on the spectinomycin-containing media, since the *Δtic20-IV* mutants exhibited almost no growth after germination (Figure 10A) (Parker et al., 2016). It should be noted that seeds sown on the spectinomycin-containing media initially possessed normal levels of chloroplast-encoded proteins including Tic214(Ycf1) and Ycf2, since they had not been exposed to spectinomycin. Tic20-IV is the only known component of the minor nonphotosynthetic-type TIC machinery (Hirabayashi et al., 2011; Nakai, 2018),

Figure 9. (continued).

(E) Displacement of bound TNP-ATP from GST-FtsHi1C_S with ATP. GST-FtsHi1C_S (0.45 μM) was preincubated with TNP-ATP (5 μM) in a cuvette to form TNP-ATP:GST-FtsHi1C_S complex (closed circles). Subsequently, indicated concentration of ATP was added into a cuvette and, after 1 min, fluorescence emission spectra were recorded (triangles, open circles).

(F) Determination of TNP-ATP:GST-FtsHi1C_S dissociation constant. Fluorescence intensities of bound TNP-ATP to GST-FtsHi1C_S (1 μM) (closed circles) and to GST (1 μM) (closed squares) as a function of TNP-ATP concentration were measured at 540 nm as in **(D)** (n = 3). Data are shown as an average of three independent measurements ± SD.

which is mainly expressed in the nonphotosynthetic tissues and functions independently from the major TIC (Tic214/100/56/20-I) complex (Kikuchi et al., 2013). The *tic20-I* knockout mutation in Arabidopsis causes albinism, seedling death, and a significantly elevated level of Tic20-IV (Hirabayashi et al., 2011). The *tic20-I tic20-IV* double knockout is embryo lethal (Hirabayashi et al., 2011; Kasmati et al., 2011).

All these observations fit our proposed model of the TIC translocation system where Tic214(Ycf1)/Tic100/Tic56/Tic20-I form the main photosynthetic-type TIC complex and, in the absence of this main TIC complex, an elevated level of Tic20-IV can partially compensate for the loss of TIC function to form a minor nonphotosynthetic alternative (Nakai, 2018). If both TIC protein translocation pathways are blocked, plants cannot grow.

As described above, FtsHi3 may form a different import motor complex that functions redundantly to the main Ycf2/FtsHi complex (Figures 1B and 3A; Supplemental Figures 3). We therefore analyzed FtsHi3 protein levels in seedlings grown on the spectinomycin-containing media, which lack *Ycf2* expression (Figures 10A to 10C). The FtsHi3 protein levels were not significantly affected by spectinomycin (Figure 10C), whereas the other Ycf2/FtsHi complex components were severely affected. Conversely, the absence of FtsHi3 (*ftshi3-KO*) only slightly affected the residual albino growth, while their protein levels of the Ycf2/FtsHi complex components were not altered, irrespective of the presence or absence of FtsHi3 (Figure 10C), suggesting that FtsHi3 might not act as an essential import motor during the residual growth in the absence of Ycf2. Other FtsHi proteins or other types of protein might instead compensate for the lack of Ycf2, inefficiently serving as an alternative import motor that presumably functions together with the above-mentioned minor Tic20-IV-containing nonphotosynthetic TIC. Elucidating such an alternative import motor may also answer why individual knockout mutations of the Ycf2/FtsHi complex components in Arabidopsis are embryo lethal, whereas those of the main TIC complex components (Tic214/Tic100/Tic56/Tic20-I) are only albino seedling lethal.

DISCUSSION

In this study, we have identified a 2-MD Ycf2/FtsHi complex in Arabidopsis and tobacco and demonstrated its essential role as a TIC-associated import motor in the translocation of preproteins across the inner envelope membrane of chloroplasts. Thus, the ATP-derived energy long known to be essential for preprotein translocation across the inner envelope membrane (Grossman et al., 1980; Theg et al., 1989; Scott and Theg, 1996; Shi and Theg, 2013) is primarily delivered via this Ycf2/FtsHi complex.

Some may argue that the Ycf2/FtsHi complex identified in this study functions as a rescue complex that removes certain arrested translocating preproteins from the TIC translocon and that the stromal Hsp70 plays a more important role in the Brownian ratchet-based translocation similar to its function in protein translocation across the inner mitochondrial membrane as was proposed previously (Liu et al., 2014). We believe this is unlikely, as the strong physical and functional associations we observed between the Ycf2/FtsHi complex and TIC, TOC, and various translocating preproteins are much greater than the relict levels of stromal Hsp70 or other chaperones associated with the preproteins in transit at the inner envelope membrane (Figures 2B and 5A, Table 1; Supplemental Figures 3 and 6C). Moreover, inclusion of ADP-AlFx in the in vitro import reactions completely blocked the preprotein translocation across the inner envelope membrane concomitant with the remarkable accumulation of the Ycf2/FtsHi complex-bound form of preproteins, whereas no such accumulation of the Hsp70-bound form could be observed (Figures 5B and 6; Supplemental Figure 8). To date, evidence has been accumulating for other hexameric ring AAA-ATPases, which couple ATP hydrolysis to polypeptide translocation through a central pore (Matyskiela et al., 2013; Gates et al., 2017; Puchades et al., 2017; Bodnar et al., 2018). The predicted pulling and translocation functions provided by the Ycf2/FtsHi complex should be investigated in detail to determine whether it can sufficiently meet the demand to act as the sole import motor, in terms of both ATP consumption and pulling speed.

Ycf2, FtsHi1, FtsHi2, FtsHi4, FtsHi5, and FtsH12 are all derived from the chloroplast genome-encoded FtsH in the ancestral cyanobacterial endosymbiont (Figure 1C; Supplemental Figures 1 and 2). Bacterial FtsHs bind to cytoplasmic membranes via two N-terminal transmembrane segments to form homo- or heterohexamers with AAA-ATPase and zinc-protease domains protruding into the cytoplasm (Okuno and Ogura, 2013). The AAA-ATPase activity of the FtsHs provides the force required to pull their substrate proteins from the membranes and push them into their protease domain for degradation (Sauer and Baker, 2011). Mitochondria also have inherited FtsH-derived proteases on their inner membranes, namely, m-AAA (Yta10/12) (Patron et al., 2018) and i-AAA (Yme1) (Puchades et al., 2017), which are also known to participate in membrane protein dislocation. Presumably, in chloroplasts, Ycf2 and the FtsHi proteins evolved to retain only the pulling function, enabling them to function in preprotein translocation as a TIC channel-associated ATP-driven import motor (Figure 1B). Endosymbiotic gene transfer and subsequent gene duplications likely gave rise to this heteromeric complex, meeting the need to accommodate a wide range of incoming preproteins. The role of FtsH12 in the complex remains unclear, but its zinc binding motif is not crucial for its essential function (Figure 7), indicating that this protein also evolved to be a Ycf2/FtsHi complex constituent and contribute to the pulling function, likely after divergence of the *Streptophyta* and *Chlorophyta* (Supplemental Figures 1 and 2). The inclusion of FtsH12 in the Ycf2/FtsHi complex as a sixth AAA subunit might have had some advantages in terms of the assembly of this heteromeric, most likely hexameric, complex. The absence of conserved hydrophobic residues in the anticipated substrate binding pore loop region of FtsH12 (Figure 1A) and the observed relatively weak cross-linking to translocating preprotein (Supplemental Figure 6C) suggest a different contribution of FtsH12 compared with the other FtsHi members in the Ycf2/FtsHi complex.

It is intriguing that the largest component of the Ycf2/FtsHi complex, Ycf2, has remained chloroplast-encoded. The seemingly simultaneous increases in the sizes of chloroplast-encoded Ycf2 and Ycf1 (Tic214) early in the evolution of the green algae (Figure 1C), and the establishment of the TIC channel and the Ycf2/FtsHi motor complex pair might be related to the high

demand for the efficient import of particular subsets of preproteins, presumably mostly photosynthetic proteins, as the *Chlorophyta* emerged (Kikuchi et al., 2013; Nakai, 2015b, 2018). The exceptionally large sizes of Ycf1(Tic214) and Ycf2 at the inner envelope membrane may facilitate efficient membrane protein translocation into the stroma and subsequent protein transfer to the thylakoids, possibly by shielding them from the lipid phase of the inner envelope membrane to prevent unfavorable trapping during translocation.

pdNAD-MDH is likely embedded in the Ycf2/FtsHi complex. We observed significantly impaired in vitro import into chloroplasts with reduced levels of this enzyme following the addition of DHAP/OAA instead of ATP. A recent report by Schreier et al. (2018) suggested that, aside from its enzymatic activity, its moonlighting role in the FtsHi/FtsH12 complex is essential for early chloroplast development, since the expression of an enzymatically inactive form of pdNAD-MDH can completely complement a knockout mutation. Overall their findings are consistent with our observations and lead to the question of why the incorporation of this enzyme into the Ycf2/FtsHi complex might be important. While we observed that reduced levels of pdNAD-MDH do not severely affect the formation and assembly of the Ycf2/FtsHi complex (Supplemental Figure 9), it might be possible that in the very early stages of chloroplast development, the inclusion of this protein in the complex is somehow essential.

The discovery of the Ycf2/FtsHi complex in this study and its complementary function with the previously identified TIC complex (Kikuchi et al., 2013) has resulted in our extensive revision of the classical TIC translocation model (Nakai, 2015a, 2018). To gain a more comprehensive understanding of the entire chloroplast protein import system, further detailed investigations are necessary from both mechanistic and evolutionary perspectives.

METHODS

Plant Materials and Growth Conditions

Arabidopsis thaliana ecotype Columbia (Col-0), Landsberg (L*er*), and Wassilewskija (Ws) were used as the wild types. For standard chloroplast isolation, in which chloroplast import activity was not compared with the mutants, Col was used. The *arc1* mutant and its complementation line *arc1 comp4* (with the 4.8-kb *FTSHi1* coding region flanked by 0.4 and 0.7 kb at the 5′ and 3′ ends, respectively, as a transgene) (Kadirjan-Kalbach et al., 2012) (gift from Katherine Osteryoung), the pdNAD-MDH microRNA line (*miR-mdh-1*) (Beeler et al., 2014) (gift from Oliver Kötting) were used. The *ftsHi3* mutant (FLAG_215F10) was obtained from INRA Versailles Arabidopsis Stock Center (Samson et al., 2002). *ftsH12* (*emb1047-1*; CS16102) and *tic20-IV* (SAIL_97_F10) (Hirabayashi et al., 2011) were obtained from the ABRC. Arabidopsis were grown on MS plates (1× Murashige and Skoog salts [Sigma-Aldrich], 1× Gamborg's B5 vitamin [Sigma-Aldrich], 2% sucrose, pH 5.8, and 0.3% phytagel [Sigma-Aldrich]) in a growth chamber under 16 h light (with fluorescent lamps at light intensity of 100–150 μmol m^{-2} s^{-1}) at 23°C/8 h dark at 21°C cycles for 18 to 22 d.

Transgenic plants for complementation analysis were generated by transformation of either the wild-type or the mutant FtsH12 cDNA under CaMV35S promoter in the pXCS vector (Witte et al., 2004) (gift from Claus-Peter Witte) into the *ftsH12* heterozygous plants by floral dip method with *Agrobacterium tumefaciens* strain GV3101(pMP90RK). AtFH12_F (5′-CCTGAATTCATTCATGGAGATTGCAATTTC-3′) and AtFH12_B (5′-CAACCCGGGCTAGCTTCTGTGGAGTGGCGC-3′), and Mu_F (5′-TATGAGGCTGGTCATATAGTGTTGGCTCAT-3′) and Mu_B (5′-AACAGCCAGAAGTCTCTTCTTTTCGTAAGA-3′) were used for the *FTSH12* cDNA amplification and the mutagenesis, respectively.

Tobacco (*Nicotiana tabacum* cv *Xanthi*) plants were grown on MS agar pots (1× Murashige and Skoog salts [Sigma-Aldrich] and 3% sucrose, pH 5.8) in a growth chamber under 16-h-light/8-h-dark cycles at 25°C for 7 to 8 weeks.

Plasmids

Expression plasmids for model preproteins, pFd-TEV-Protein A (pFd-TEV-ProtA) and pSSU-TEV-Protein A (pSSU-TEV-ProtA) were previously constructed (Kikuchi et al., 2013) from the corresponding original plasmids (Schnell et al., 1994) (gift from D. Schnell). These model preproteins consist of either the precursor of ferredoxin (pFd) or that of Rubisco small subunit (pSSU) fused to the N terminus of the IgG binding domain of staphylococcal protein A, carrying a TEV protease cleavage site (SENLYFQGELKT) between each preprotein and the protein A domain as well as a C-terminal hexahistidine-tag. Plasmids for $pSSU_{FLAG}$-TEV-Protein A (pSSU*-TEV-ProtA) and pFd_{FLAG}-TEV-Protein A (pFd*-TEV-ProtA) were generated by inserting a DNA fragment consisting of 5′-CCGATTATAAAGATCATGATGGCGATTATAAAGATCATGATATCGATTATAAAGATGATGATGATAAAA-3′ and 5′-CTAGTTTTATCATCATCATCTTTATAATCGATATCATGATCTTTATAATCGCCATCATGATCTTTATAATCGGTGCA-3′ corresponding to 3xFLAG sequence (DYKDHDGDYKDHDIDYKDDDDK) into the *Nsi*I-*Spe*I site of pSSU-TEV-ProtA or pFd-TEV-ProtA plasmid, between the pSSU or pFd and the TEV cleavage site, respectively. Expression plasmids for $pL11_{FLAG}$-TEV-Protein A (pL11*-TEV-ProtA), $pLHCP_{FLAG}$-TEV-Protein A (pLHCP*-TEV-ProtA), and $OEP7_{FLAG}$-TEV-Protein A (OEP7*-TEV-ProtA) were generated by replacing the *Nhe*I-*Bam*HI pFd-coding DNA fragment of pFd_{FLAG}-TEV-Protein A either with a PCR-amplified cDNA fragment encoding the precursor of chloroplast-localized ribosomal subunit L11 (pL11), with that encoding the precursor of light-harvesting chlorophyll binding protein (pLHCP) or with that encoding the entire Arabidopsis outer envelope membrane protein OEP7 (Lee et al., 2001), respectively. Primers used for PCR amplifications are as follows: PRPL_F, 5′-CCTGCTAGCTCTTCTCTATCAACTCTTTGC-3′; PRPL_B, 5′-CCAGGATCCTAAAACTGCTTTCTTTTTGGG-3′; pLHCP_F, 5′-CCTGCTAGCTCATCATCATCCATGGCTCTC-3′; pLHCP_B, 5′-CCAGGATCCTCCGGGAACAAAGTTGGTGGC-3′; ATOEP7_F, 5′-CCTGCTAGCATGGGAAAAACTTCGGGAGCG-3′; and ATOEP7_B, 5′-CCAGGATCCCAAACCCTCTTTGGATGTGGT-3′. The plasmid for pFd_{FLAG}-DHFR-TEV-Protein A was generated by inserting a PCR-amplified cDNA fragment encoding mouse dihydrofolate reductase (DHFR) using primers DHFR_F (5′-CCTGCTAGCGGATCCGGCATCATGGTTCG-3′) and DHFR_B (5′-CCATCTAGAGTCTTTCTTCTCGTAGACTTC-3′). The plasmid for $pSSU_{FLAG}$ was generated by removing the DNA fragment corresponding to TEV-Protein A from $pSSU_{FLAG}$-TEV-Protein A. All the above-mentioned plasmids were constructed either in the pET21a or pET24a expression vector backbone (Novagen) carrying a T7 promoter for expression. Construction of plasmids pFNR (Hirohashi et al., 2001) and pSSU-DHFR (Kikuchi et al., 2009) was described previously. For expression of the long form (amino acids 417–946) (FtsHi1C_L) and the short form (amino acids 417–684) (FtsHi1C_S) of the C-terminal domain of Arabidopsis FtsHi1 as a fusion protein with GST (from *Schistosoma japonicum*), the corresponding cDNA fragments were PCR-amplified and cloned into pCold-GST vector (Takara) and modified by KOD One PCR enzyme (Toyobo). The following primers were used: sFL1_F, 5′-CCTCTCGAGGCAGAAGCTCGTGTTGATGGT-3′;

sFL1_B, 5′-CCAAAGCTTACGTGTCGGACCAACAGTGAG-3′; sFL1_R2, 5′-CCAAAGCTTTCATACTTGAGCATTGACGTC-3′; arc1_F, 5′-GAGCTAAGGTAAACAAGCCATTCGTTATTTTCATCGATGAAATTG-3′; and arc1_B, 5′-CAATTTCATCGATGAAAATAACGAATGGCTTGTTTACCTTAGCTC-3′. Expression in *Escherichia coli* cells [BL21(DE3) Star; Novagen] was induced at 15°C overnight according to the manufacturer's instructions, and the recombinant proteins were purified with nickel chelate chromatography using Ni-Sepharose (GE Healthcare).

Preparation of Antibodies and Immunoblotting

To obtain antisera specific for each FtsH-like protein used in this study, their C-terminal regions with relatively low sequence similarities were used as antigens. Corresponding cDNA fragments were amplified as previously described with the following primers: FtsHi1 (amino acids 610–946), FL1C_F, 5′-CCTGGATCCGCGAAAGGGAGATTGGATATT-3′, FL1C_B, 5′-CCAGTCGACTCATACTTGAGCATTGACGTC-3′; FtsHi2 (amino acids 548–876), FL2C_F, 5′-CCTGGATCCGGAGAGGTCATCACCATTGCT-3′, FL2C_B, 5′-CCACTCGAGTTATGAACTGTTTCTTGCGGT-3′; FtsHi3 (amino acids 181–622), FL3C_F, 5′-CCTGGATCCGTTACGAATCTTCGAGGTGGT-3′, FL3C_B, 5′-CCAGTCGACTTAGCTGAGAGTTTGATAACC-3′; FtsHi4 (amino acids517–855),FL4C_F,5′-CCTCATATGCAAGAAGTAGCTGAGAACACG-3′, FL4C_B, 5′-CCAGTCGACTTAAAAGAAATGGGTTGCCAT-3′; FtsHi5 (amino acids 1003–1320), FL5C_F, 5′-CCTCTCGAGGCTCTCGAAAGTAGTGCCTTC-3′, FL5C_B, 5′-CCAAAGCTTTTAGGTTGGTGCACTAAGAAG-3′; FtsH12 (amino acids 741–1008), F12_F, 5′-CCTCTCGAGGGTATGGGTGTACTTCTTACA-3′, F12_B, 5′-CCAAAGCTTTTAGGTTGGTGCACTAAGAAG-3′. For antigens of the N-terminal (amino acids 320–837) and the C-terminal (amino acids 1674–1812) fragments of Arabidopsis Ycf2, the following primers were used: Y2_F1_Nde, 5′-CCTCATATGTGGCAATTCCACCAAGATCTC-3′, Y2_B1_XhoI, 5′-CCACTCGAGACGGCTCTTCCGCTCAGAAAC-3′, Y2_F2_NdeI, 5′-CCTCATATGCTGAACAAGTTCCTGGATAAC-3′, Y2_B2_XhoI, 5′-CCACTCGAGTCGATCCAATAGCGTTCCGTT-3′. For antigen against a Tgd4-like protein (At2g44640) (amino acids 1–451), the following primers were used: 4640_F, 5′-CCTCATATGGCGAATCTTAACTCAGCTATT-3′, 4640_B, 5′-CCACTCGAGAAACTCAAAAACTCGGAGCTC-3′. The amplified fragments were separately cloned into a pColdI vector (Takara) and used for overexpression with an N-terminal hexahistidine-tag in *E. coli* BL21(DE3) cells (Novagen). Recombinant proteins were purified with nickel chelate chromatography and were injected into rabbits.

Preparation of antibodies against Arabidopsis Tic214 (AtTic214), AtTic100, AtTic56, PsToc75, PsToc159 (86C), PsTic110, PsHsp93, and SoHsp70 was described previously (Asakura et al., 2004; Kikuchi et al., 2006, 2013). Antibodies against Arabidopsis pdNAD-MDH, Tic40, and Var2 (gifts from Renate Scheibe, Hsou-min Li, and Wataru Sakamoto, respectively), and monoclonal antibodies against 3xFLAG tag (clone M2, F1804; Sigma-Aldrich) and HA tag (clone HA-7, Sigma-Aldrich; clone 16B12, BioLegend) were used. Immunoblotting was performed as described previously with ECL Prime detection kits (GE Healthcare). To avoid aggregations, almost all samples were denatured in Laemmli sample buffer at 37°C for 30 min prior to electrophoresis. Ycf2 and FtsHi family proteins were separated by 6.5% SDS-PAGE.

Generation of Tobacco Transgenics

The pBluescript II(KS+)-based vector Prrn-aadA/pBSII carrying the selectable marker gene *aadA* driven by the tobacco plastid 16S rRNA promoter (P*rrn*) was used for construction of plasmids to generate tobacco transgenics. The plastid DNA fragments corresponding to the C-terminal regions of Ycf1 and Ycf2 were obtained by PCR-amplification using the following primers: NtY1_C_F3_BamHI, 5′-CCTGGATCCAAAGAACCCGCAAGTCAAGGA-3′; NtY1_C_B_XmaI, 5′- GGACCCGGGATTTATTTTCAATTGTGGATACATATGTATCC-3′; Y2_C_F_BamHI, 5′- CCTGGATCCAGTTGTTCTGCCGGATCGGTC-3′; Y2_C_B_XmaI, 5′- GGACCCGGGCATGAATCCAATTTTCATTTCATCCGG-3′. The DNA cassette corresponding to the C-terminal tandem HA tag/StrepII tag (PG-GYPYDVPDYAVGAGWSHPQFEK*) derived from pXCS-HAStrep (Witte et al., 2004) was introduced as an *Xma*I/*Xba*I fragment, 5′-CCCGGGGGTTATCCATACGATGTTCCAGATTATGCTGTCGGCGCCGGTTGGTCTCATCCTCAATTTGAAAAATAAGTCTAGA-3′. The resulting plasmids, pY1C and pY2C, were used for plastid transformation.

Plastid transformation was performed as described previously (Svab and Maliga, 1993) with slight modifications. Young leaves from sterile tobacco plants were bombarded with plasmid DNA-coated gold particles (0.6 μm) at a pressure of 1100 p.s.i. using the Biolistic PDS 1000/He particle delivery system (Bio-Rad). Antibiotic-resistant shoots/calli were selected on the RMOP agar medium consisting of MS salts, 3% sucrose, 0.1 mg/L of 1-naphthaleneacetic acid, 1 mg/L of N^6-benzyladenine, 1 mg/L of thiamine, and 100 mg/L of inositol, supplemented with 200 mg/L of spectinomycin dihydrochloride. Targeted integration of transgenes was confirmed by genomic PCR. The resulting transplastomic lines were subjected to several rounds of regeneration to increase homoplasmy. Finally, for each construct, three independent nearly homoplasmic lines were rooted on MS agar medium supplemented with 3% sucrose and 500 mg/L of spectinomycin dihydrochloride. The T0 plants were propagated by in vitro meristem culture on the MS selection medium.

DNA extraction and genomic PCR were performed as follows. A small piece of transgenic shoots or leaves (~0.5 cm^2) was put in a 1.5-mL microtube. The tissue was homogenized in 100 μL DNA extraction buffer (200 mM Tris-HCl, pH 7.5, 250 mM NaCl, 25 mM EDTA, and 0.5% SDS) using pellet pestles cordless motor (Sigma-Aldrich) and extracted by phenol:chloroform:iso-amylalcohol (25:24:1). After centrifugation, the supernatant was subjected to ethanol precipitation. The resultant pellet containing total plant DNA was resuspended in 30 μL sterile water and used as the PCR template. The genomic PCR was conducted using the following primers: NY1-1_1F, 5′-ACCAAACTAATCAAAGATACCCCG-3′; NY1-1_1R, 5′-AATAAGCTAGGAGTCGTTGACGT-3′; YCF2-Fd2, 5′-GGTCATTTCGGGGCAAGCGGATCATTTATG-3′; YCF2-Rv2, 5′-ATGCCCGCCCGTAACCCAGCAGATAAAG-3′;HA-Fd1,5′-CCCGGGGGTTATCCATACGATGTTCC-3′; aadA-Rv2, 5′-GGACAAATTCTTCCAACTGATCTGCGC-3′.

Isolation of Chloroplasts

Intact chloroplasts from Arabidopsis or tobacco were isolated by homogenization method as described previously (Svab and Maliga, 1993; Bruce et al., 1994; Kikuchi et al., 2006) with the following modifications. Aerial plant tissues weighing from 30 to 60 g were homogenized in 2 liters (330 mL × 6 times) of blending buffer (50 mM HEPES-KOH, pH 7.8, 330 mM sorbitol, 2 mM EDTA, 1 mM $MgCl_2$, 50 mM sodium ascorbate, and 0.25% BSA) in a Waring blender equipped with disposable razor blades. The homogenate was filtered through four layers of Miracloth (Calbiochem) and then centrifuged at 4000*g* for 3 min. The crude chloroplast pellet was resuspended in HS buffer (50 mM HEPES-KOH, pH 7.8, and 330 mM sorbitol) and overlaid onto a step gradient, composed of 30% and 80% Percoll in HS buffer. A chloroplast band that appeared at the boundary between 30% and 80% Percoll was collected, washed, and kept on ice in the dark until use.

Purification of the Tobacco Ycf2 and Ycf1 Complexes

Intact tobacco chloroplasts carrying HA-tagged Ycf2 or Ycf1 were isolated as described above. To purify individual complexes, the tobacco chloroplast pellet was directly solubilized with 1% Triton X-100, 100 mM Tris-HCl, pH 8.0, 10% (w/v) glycerol, 300 mM NaCl, 5 mM EDTA, and 1% (v/v) protease inhibitor cocktail (for plant extracts, P-9599; Sigma-Aldrich) to a final concentration of 2 mg chlorophyll/mL for 30 min, and

insoluble material was removed by ultracentrifugation. The resulting 1.5 mL supernatant was incubated with anti-HA agarose (30 μL, packed volume, A2095; Sigma-Aldrich) for 5 h in cold room (6°C) with end-over-end mixing. The beads were washed five times with wash buffer (0.1% Triton X-100, 100 mM Tris-HCl, pH 8.0, 300 mM NaCl, and 1 mM EDTA). Bound Ycf2 or Ycf1 complexes were eluted with 1 mg/mL HA peptide in wash buffer. Where indicated, dodecylmaltoside was used instead of Triton X-100 as detergent throughout the purification with varying concentrations of salts. For BN-PAGE, prior to loading, the eluate was mixed with glycerol and CBB-G at final concentrations of 10% (w/v) and 0.12%, respectively. For SDS-PAGE, the eluted protein complexes were denatured with 2% SDS and 50 mM tris(2-carboxyethyl)phosphine hydrochloride (TCEP) at 37°C for 30 min.

LC-MS/MS Analysis

The purified tobacco Ycf2-HA complex was separated by 2D-BN/SDS-PAGE. Proteins were visualized by silver staining, and the 32-kD protein band was excised from the gel. After treatment with DTT for reduction and with iodoacetamide for alkylation, in-gel digestion using trypsin was performed on a ProGest (Genomic Solutions) workstation. The digested samples were analyzed by nano-LC-MS/MS with a 30 min gradient on an LTQ-Orbitrap XL (Thermo Fisher Scientific). Product ion data were searched against the Uniprot-N-tabacum database and the tobacco translated EST database using the MASCOT search engine with the following parameters: peptide mass tolerance, 10 ppm; fragment mass tolerance, 0.5 D; trypsin as enzyme allowing up to two missed cleavages; carboxymethylation on cysteines as a fixed modification, oxidation on methionines, deamidation on asparagines, and an N-terminal pyroglutamine as variable modifications. The Scaffold program v.4.3.2 was used to validate the MASCOT output data. Peptide identifications were accepted if they could be established at greater than 99.0% probability as specified by the Peptide Prophet algorithm. Protein identifications were accepted if they could be established at >99.9% probability and finally filtered based on the criteria; number of top matches = 1.

For LC-MS/MS analysis of the purified translocation intermediates, after alkylation with iodoacetamide, the samples were digested with trypsin in solution and analyzed by UltiMate 3000 Nano LC systems coupled to Q-Exactive hybrid quadrupole-Orbitrap mass spectrometer (Thermo Fisher Scientific). Peptides and proteins were identified by MASCOT search against the Uniprot-Arabidopsis-thaliana database as above.

Enzymatic Assay of NAD-MDH

NAD-MDH (EC 1.1.1.37) activity was assayed spectrophotometrically as described previously (Sjögren et al., 2014) by measuring NADH oxidation at 340 nm at 25°C in 50 mM HEPES-KOH, pH 7.8, 10 mM $MgCl_2$, 0.05% Triton X-100 with 0.15 mM OAA, and 0.1 mM NADH as substrates. The specific activity of pdNAD-MDH in the purified Ycf2-HA complex was calculated to be ~1.1 mmol of NADH (oxidized) per mg of protein per min (n = 3).

Purification of the Translocation Intermediates

Isolated intact chloroplasts were incubated with 100 to 200 nM urea-denatured Protein A-tagged preprotein in HS buffer containing 0, 0.5, or 3 mM Mg-ATP, 5 mM $MgCl_2$, and 5 mM DTT for 10 min at 25°C in the dark. The reactions were terminated by chilling and centrifugation, and chloroplasts were washed twice with HS buffer. The chloroplast pellet was directly solubilized with 1% digitonin in TGS buffer (50 mM Tris-HCl, pH 7.5, 10% [w/v] glycerol, and 250 mM NaCl) in the presence of 5 mM EDTA, 5 mM DTT, and 0.5% (v/v) protease inhibitor cocktail to a final concentration of 1 mg chlorophyll/mL for 20 min, and insoluble material was removed by ultracentrifugation. The 1- to 1.5-mL supernatant was incubated with IgG Sepharose (15 μL, packed volume) for 2 to 3 h in a cold room (6°C) with end-over-end mixing. Commercial IgG-Sepharose used here was further cross-linked with dimethyl pimelimidate to avoid leakage of IgG during the cleavage step. The beads were washed three times with 1 mL and twice with 0.5 mL of 0.5% digitonin in TGS buffer, in which the third wash was performed with end-over-end mixing for 5 min in cold room, and in which the fourth wash, the resuspended beads were transferred to a new 0.5-mL siliconized tube to facilitate washing. Bound translocation intermediate complexes were eluted under nondenaturing conditions by cleavage with AcTEV protease for 1 h at 24°C with end-over-end mixing. The eluted protein complexes were denatured with 2% SDS and 50 mM TCEP at 37°C for 30 min for SDS-PAGE.

For purification of preprotein-interacting proteins after DSP cross-linking, tobacco intact chloroplasts carrying HA-tagged Ycf1 and $pL11_{FLAG}$-TEV-Protein A were used. After accumulation of translocation intermediates in the presence of 0.5 mM ATP, chloroplasts were incubated with 0.1 mM DSP (Thermo Fisher Scientific). After quenching by the addition of 10 mM glycine, chloroplasts were completely solubilized and denatured in 1% SDS-containing buffer. After dilution with excess Triton X-100-containing buffer, $pL11_{FLAG}$-TEV-Protein A and its directly cross-linked proteins were purified with IgG-Sepharose and analyzed as described above.

Binding and Chase Experiments Using the Short Preprotein, $pSSU_{FLAG}$

To make early translocation intermediates, nonradiolabeled $pSSU_{FLAG}$ was synthesized in cell-free in vitro translation system using *E. coli* S30 extract (L1110; Promega). Arabidopsis chloroplasts were incubated with $pSSU_{FLAG}$ in HS buffer containing 0.1 mM Mg-ATP, 5 mM $MgCl_2$, and 5 mM DTT for 10 min at 25°C in the dark to form an early translocation intermediate. After centrifugation, resuspended chloroplasts were supplemented with or without 0.2 mM ADP, 5 mM NaF, and 0.2 mM $AlCl_3$ to form ADP-AlFx and were incubated for 3 min at 25°C in the dark. The chloroplasts were further supplemented with or without 3 mM ATP, and the import reaction was chased for another 20 min at 25°C in the dark. Each reaction contained chloroplasts equivalent to 1 mg chlorophyll in a volume of 3 mL. The reaction was terminated by chilling and centrifugation, and the chloroplast pellet was frozen in liquid nitrogen and stored at −80°C. The chloroplast pellet was solubilized with 1% digitonin in TGS buffer in the presence of 5 mM EDTA and 0.5% (v/v) protease inhibitor cocktail and the absence of DTT to a final concentration of 1 mg chlorophyll/mL for 20 min. After insoluble material was removed by centrifugation, the 1 mL supernatant was incubated with anti-FLAG M2 affinity gel (15 μL, packed volume, A2220; Sigma-Aldrich) for 3 h in cold room with end-over-end mixing. The beads were washed five times with 0.2% digitonin in TGS buffer as described above. Bound translocation intermediate complexes were eluted with 0.1 mg/mL 3xFLAG peptide in TGS buffer containing 0.2% digitonin. The eluted protein complexes were denatured as described above, followed by SDS-PAGE and immunoblotting.

In Vitro Translation of Radiolabeled Preproteins and Chloroplast Import Assay

Radiolabeled preproteins were synthesized in vitro using a coupled transcription-translation system (TNT T7 Quick for PCR DNA, L5540; Promega), in the presence of [^{35}S]Met. Chloroplast import assay of [^{35}S]-labeled preproteins was performed as described previously (Kikuchi et al., 2009). Import assays were performed in at least three individual chloroplast isolations.

Site-Specific Cross-Linking and Reciprocal Coimmunoprecipitation

The expression plasmid for the cysteine-less model ferredoxin preprotein carrying HA-tag, pFdvari-HA(ΔC) was constructed by inserting the following synthetic gene into the pET-24a (Novagen): 5′-ATGGCAAGCACCCTGAGTACCCTGAGCGTTAGCGCAAGCCTGCTGCCGAAACAGCAGCCGATGGTTGCAAGCAGCCTGCCGACCAATATGGGTCAGGCACTGTTTGGTCTGAAAGCAGGTAGCCGTGGTCGTGTTACCGCAAGCGCAACCTATCGTGTGACCCTGATTACCCGTGAAAGCGGCACCGTTACCTTTGATAGTCCGGATGATGTTTATGTTCTGGATCAGGCAGAAGAAGAAGGTATTGATCTGCCGTATAGCAGCCGTGCAGGTAGCAGCAGCAGCTCAGCAGGTCGTGTTGTTGCCGGTAGCGTGGATCAGAGCGATCAGAGTTTTCTGGATGATGATCAGATTGAAGCAGGTTGGGTTCTGACCGATAATGTTCGTCAGGTTCAGAGCACCTATCCGTATGATGTTCCGGATTATGCGGGATCC-3′. The codons for Ser residues at the sixth and the ninth positions in the transit peptide were individually mutated to the Cys codon using the following pairs of primers with KOD Plus Mutagenesis Kit (Toyobo): pFdvari-HA(6C), 5′-TGCAGTACCCTGAGCGTTAGCGCAAGCCTG-3′ and 5′-GAGGGTGCTTGCCATGGTATATCTCCTTCT-3′; pFdvari-HA(9C), 5′-TGCAGCGTTAGCGCAAGCCTGCTGCCGAAA-3′ and 5′-GAGGGTACTCAGGGTGCTTGCCATGGTATA-3′. Purified preproteins were treated with 40 mM DTT just prior to use. Import experiments were performed essentially as described above. To deplete internal ATP, chloroplasts were first preincubated with 400 nM nigercin (Sigma-Aldrich) and 2 mM D-glyceric acid (Sigma-Aldrich) for 10 min at 25°C. After import, chloroplasts were washed twice with HS buffer and subjected to cross-linking with 1 mM BMH (Thermo Fisher Scientific) in HS buffer at 25°C for 10 min in the dark. After quenching with 10 mM DTT in HS buffer on ice for 20 min, chloroplasts were washed twice with 30 mM DTT in HS buffer and once with HS buffer containing 0.1% protease inhibitor cocktail (Sigma-Aldrich).

BMH-treated chloroplasts were solubilized in 1% (w/v) SDS, 50 mM Tris-HCl, pH 7.5, 1 mM EDTA, and 5% (v/v) cOmplete protease inhibitor cocktail (Roche) at 3 mg chlorophyll/mL for 20 min at room temperature, and insoluble materials were removed by centrifugation. The resulting supernatant was diluted 20-fold with Triton X-100 trap buffer (1% [v/v] Triton X-100, 50 mM Tris-HCl, pH 7.5, 150 mM NaCl, 1 mM EDTA, and 0.1% protease inhibitor cocktail [Roche]). Immunoprecipitation was performed using IgG-conjugated Protein A-Sepharose (GE Healthcare) as described previously. For this purpose, specific antibodies were selected from crude antisera using antigen-conjugated Sepharose (NHS-activated Sepharose FF; GE Healthcare). To eliminate any potential cross-reactions between the selected antibodies and the preproteins, IgGs were further incubated with pFdvari-HA(ΔC)-conjugated Sepharose, and unbound IgGs were used for conjugation to Protein A-Sepharose. The anti-HA agarose (A2095; Sigma-Aldrich) was also used for reciprocal immunoprecipitations. The anti-HA-tag antibodies (Anti-HA.11, 901514; BioLegend) were used for immunodetection.

Modification with PEG-Mal

Inverted inner envelope membrane vesicles were prepared as described previously (Keegstra and Yousif, 1986). The envelope vesicles (1.44 μg proteins) were resuspended in TE buffer (10 mM Tricine, pH 7.5, and 2 mM EDTA) containing 0.2 M sucrose, 2 mM TCEP, and 5 mM $CaCl_2$. Where indicated, 0.2% dodecylmaltoside was included in the buffer to solubilize membranes. After the envelope vesicles were incubated with or without 20 μg/mL thermolysin for 30 min on ice, proteolysis was quenched by adding 20 mM EDTA and 133 μM phosphoramidon (specific inhibitor of thermolysin). Then, the envelope vesicles were reacted with or without 3 mM PEG-Mal, a membrane-impermeable thiol-alkylation reagent, at 25°C for 20 min. Finally, PEG-Mal modification reaction was quenched by adding 30 mM DTT. The envelope vesicle suspension was directly dissolved in Laemmli sample buffer and analyzed by 6.5% SDS-PAGE and immunoblotting. In the case of pdNAD-MDH modification, one-tenth diluted stroma was added to one reaction to compare with pdNAD-MDH present in the envelope fraction. This sample was separated by 5 to 10% WIDE-RANGE gel (Nacalai Tesque).

Nucleotide Binding Assays

Fluorescent measurements of TNP-ATP (Santa Cruz Biotechnology) were conducted at 25°C in assay buffer (50 mM Tris-HCl, pH7.5, 50 mM NaCl, and 0.1 mM EDTA) using 1-cm pathlength cuvettes in an F-7000 fluorescence spectrophotometer (Hitachi High-Tech Science). Fluorescence was recorded using a 410-nm excitation wavelength from 500 to 600 nm. In all assays, fluorescence from the reference measurements with the buffer containing the corresponding concentration of TNP-ATP and those with the buffer containing proteins but no added TNP-ATP were subtracted as background. For saturation binding experiments at protein concentration of 1 μM, concentrated TNP-ATP stocks were added stepwise covering a range of 0.5 to 10 μM concentrations. For displacement experiments at protein concentration of 0.45 μM, the initial concentration of TNP-ATP was fixed at 5 μM, and ATP was titrated covering a range of 50 to 500 μM. In all cases, concentrated stocks of nucleotides were added to 2 mL of reaction mixture ensuring that the total added volume did not exceed 1.1% of the total reaction volume.

Phylogenetic Analysis

To understand the evolutionary process of Ycf2 and FtsH-like proteins in plants, a phylogenetic tree of these proteins was inferred. Entire C-terminal sequences starting from the Walker A motif (plus relatively conserved flanking upstream 11 amino acids) were used for phylogenetic analysis. Amino acid sequences of these proteins were aligned using the program T-COFFEE (Notredame et al., 2000). Phylogenetic trees of these proteins were constructed using the maximum likelihood (ML) and the Bayesian methods, independently. The best-fit substitution model was selected based on Akaike information criterion using the AMINOSAN program in the KAKUSAN4 software package (Tanabe, 2007). The ML tree with the LG + Γ model was searched by the rapid-bootstrap option implemented in RAxML program version 8.1.5 (Stamatakis, 2014). The reliability of the ML tree nodes was assessed by the rapid bootstrap method with 100 replicates. The Bayesian tree was reconstructed using MrBayes 3.2.6 (Ronquist et al., 2012). In the Bayesian phylogenetic analysis, the Markov chain Monte Carlo process was set so that four chains (three heated and one cold) ran simultaneously. We continued the runs for 1,000,000 cycles to confirm lack of improvement in the likelihood scores, with one in every 500 trees being sampled. Posterior probabilities for internal branches were estimated using 900,000 cycles (1800 trees) after reaching stationary in the log likelihood scores. The resulting phylogenetic trees and the associated multiple sequence alignment are shown in Supplemental Figures 1 and 2 and Supplemental File 1.

Statistical Analysis

For investigations of difference in import efficiency of mutant chloroplasts, experiments were replicated (biological replicates) at least three times. Other experiments were performed in at least two biological replicates and at least two technical replicates. In data shown in Figures 8G and 9F, error bars represent SE and SD, respectively, and were calculated from triplicate biological and technical replicates, respectively. Using a two-tailed, paired *t* test, differences were considered statistically significant at $P < 0.01$.

Miscellaneous

Generation of the transgenic plant overexpressing Protein A-tagged Tic20 (PA2-TIC) was described previously (Kikuchi et al., 2013). 2D-BN/

SDS-PAGE was performed as described previously (Kikuchi et al., 2011). Integration of $OEP7_{FLAG}$-TEV-Protein A was assessed by alkaline extraction with 0.1 M Na_2CO_3, pH 11.5, followed by ultracentrifugation. Radiolabeled proteins in dried gels were detected using a BAS-2000II image analysis system (Fujifilm) and quantified using Image Gauge version 3.45 software (Fujifilm). Stained gels and immunoblots were scanned with a scanner (GT-9700F; Epson), and the amounts of protein bands were quantified using ImageJ software (NIH).

Accession Numbers

Sequence data from this study can be found in The Arabidopsis Information Resource database under the following accession numbers: YCF2 (AtCg00860), FtsHi1 (At4g23940), FtsHi2 (At3g16290), FtsHi4 (At5g64580), FtsHi3 (At3g02450), FtsHi5 (At3g04340), FtsH12 (At1g79560), pdNAD-MDH (At3g47520), Tic20-I (At1g04940), Tic20-IV (At4g03320), Tic56 (At5g01590), Tic100 (At5g22640), and Tic214 (Ycf1) (AtCg01130).

Supplemental Data

Supplemental Figure 1. Bayesian phylogenetic tree of Ycf2 and FtsH-like proteins.

Supplemental Figure 2. Maximum likelihood phylogenetic tree of Ycf2 and FtsH-like proteins in cyanobacteria (blue), *Rhodophyta* (magenta), *Chlorophyta* (light green), and *Streptophyta* (land plants, green).

Supplemental Figure 3. Association of various translocating preproteins with the Arabidopsis Ycf2 and FtsH-like proteins.

Supplemental Figure 4. Generation of transplastomic tobacco lines expressing C-terminal HA-tagged Ycf2 or Ycf1 proteins and specificities of various antibodies.

Supplemental Figure 5. LC-MS/MS identification of pdNAD-MDH from *Nicotiana tabacum* and multiple sequence alignment with NAD-MDH isoproteins from *Arabidopsis thaliana*.

Supplemental Figure 6. Association of the tobacco Ycf2/FtsHi complex components with various translocating preproteins.

Supplemental Figure 7. The membrane topology of the Ycf2/FtsHi complex components in the inner envelope membrane of Arabidopsis chloroplasts.

Supplemental Figure 8. Direct involvement of the Ycf2 in transit-peptide recognition during preprotein translocation.

Supplemental Figure 9. In vivo and in vitro analysis of the pd-NAD-MDH-silencing Arabidopsis mutant.

Supplemental Figure 10. FtsHi3-lacking chloroplasts exhibit normal rates of in vitro import of various preproteins.

Supplemental Data Set 1. Identified peptides of the translocation intermediate-associating proteins by LC-MS/MS.

Supplemental File 1. Multiple sequence alignment of Ycf2 and FtsH-like protein sequences.

ACKNOWLEDGMENTS

This article is dedicated to the memory of Professor Kentaro Inoue, whose critical reading, thoughtful comments, and encouragement are greatly appreciated. We thank K.W. Osteryoung, O. Kötting, R. Scheibe, W. Sakamoto, C.-P. Witte, H.-M. Li, and D. Schnell for materials and A. Nakamura for technical help. We also thank T. Schreier and colleagues for sharing their unpublished work and thoughts. This work was supported by the Ministry of Education, Culture, Sports, Science, and Technology KAKENHI (26117712, 24117511, 15H01535, 17H05668, and 17H05725 to M.N.; 15H01236 to T.S.) and by Japan Society for the Promotion of Science KAKENHI (26291060 and 26650017 to M.N., 15K14912 to Yo.N., 15K14553 and 25291065 to T.S., and 16K07400 to Y.A.).

AUTHOR CONTRIBUTIONS

S.K., Y.A., M.I., Y.K., J.B., Y.H.-I., Yu.N., and M.N. carried out biochemical analyses. M.I., Yo.N., S.K., and M.N. performed genetic analyses. Yo.N., T.S., and M.N. established transgenic tobacco plants. Y.H., Yu.N., and M.N. performed phylogenetic analyses. K.T., H.M., Y.H.-I., and M.N. carried out the mass spectrometric analyses. M.N. conceived and designed the whole project and wrote the manuscript with the input of other authors.

Received May 7, 2018; revised August 16, 2018; accepted October 1, 2018; published October 11, 2018.

REFERENCES

Asakura, Y., Hirohashi, T., Kikuchi, S., Belcher, S., Osborne, E., Yano, S., Terashima, I., Barkan, A., and Nakai, M. (2004). Maize mutants lacking chloroplast FtsY exhibit pleiotropic defects in the biogenesis of thylakoid membranes. Plant Cell **16:** 201–214.

Beeler, S., Liu, H.C., Stadler, M., Schreier, T., Eicke, S., Lue, W.L., Truernit, E., Zeeman, S.C., Chen, J., and Kötting, O. (2014). Plastidial NAD-dependent malate dehydrogenase is critical for embryo development and heterotrophic metabolism in Arabidopsis. Plant Physiol. **164:** 1175–1190.

Bodnar, N.O., Kim, K.H., Ji, Z., Wales, T.E., Svetlov, V., Nudler, E., Engen, J.R., Walz, T., and Rapoport, T.A. (2018). Structure of the Cdc48 ATPase with its ubiquitin-binding cofactor Ufd1-Npl4. Nat. Struct. Mol. Biol. **25:** 616–622.

Boudreau, E., Turmel, M., Goldschmidt-Clermont, M., Rochaix, J.-D., Sivan, S., Michaels, A., and Leu, S. (1997). A large open reading frame (orf1995) in the chloroplast DNA of *Chlamydomonas reinhardtii* encodes an essential protein. Mol. Gen. Genet. **253:** 649–653.

Bruce, B.D., Perry, S., Froehlich, J., and Keegstra, K. (1994). In vitro Import of Proteins into Chloroplasts. In Plant Molecular Biology Manual, S.B. Gelvin, and R.A. Schilperoot, eds (Dordrecht: Springer), pp. 1–15.

Cvetić, T., Veljović-Jovanović, S., and Vucinić, Z. (2008). Characterization of NAD-dependent malate dehydrogenases from spinach leaves. Protoplasma **232:** 247–253.

Drescher, A., Ruf, S., Calsa, T., Jr., Carrer, H., and Bock, R. (2000). The two largest chloroplast genome-encoded open reading frames of higher plants are essential genes. Plant J. **22:** 97–104.

Ferro, M., et al. (2010). AT_CHLORO, a comprehensive chloroplast proteome database with subplastidial localization and curated information on envelope proteins. Mol. Cell. Proteomics **9:** 1063–1084.

Flores-Pérez, Ú., Bédard, J., Tanabe, N., Lymperopoulos, P., Clarke, A.K., and Jarvis, P. (2016). Functional analysis of the Hsp93/ClpC chaperone at the chloroplast envelope. Plant Physiol. **170:** 147–162.

Gates, S.N., et al. (2017). Ratchet-like polypeptide translocation mechanism of the AAA+ disaggregase Hsp104. Science **357:** 273–279.

Grossman, A., Bartlett, S., and Chua, N.-H. (1980). Energy-dependent uptake of cytoplasmically synthesized polypeptides by chloroplasts. Nature **285:** 625–628.

Hirabayashi, Y., Kikuchi, S., Oishi, M., and Nakai, M. (2011). In vivo studies on the roles of two closely related Arabidopsis Tic20 proteins, AtTic20-I and AtTic20-IV. Plant Cell Physiol. **52:** 469–478.

Hirohashi, T., Hase, T., and Nakai, M. (2001). Maize non-photosynthetic ferredoxin precursor is mis-sorted to the intermembrane space of chloroplasts in the presence of light. Plant Physiol. **125:** 2154–2163.

Huang, P.-K., Chan, P.-T., Su, P.-H., Chen, L.-J., and Li, H.-M. (2016). Chloroplast Hsp93 directly binds to transit peptides at an early stage of the preprotein import process. Plant Physiol. **170:** 857–866.

Inoue, H., Li, M., and Schnell, D.J. (2013). An essential role for chloroplast heat shock protein 90 (Hsp90C) in protein import into chloroplasts. Proc. Natl. Acad. Sci. USA **110:** 3173–3178.

Jackson, D.T., Froehlich, J.E., and Keegstra, K. (1998). The hydrophilic domain of Tic110, an inner envelope membrane component of the chloroplastic protein translocation apparatus, faces the stromal compartment. J. Biol. Chem. **273:** 16583–16588.

Jarvis, P., and López-Juez, E. (2013). Biogenesis and homeostasis of chloroplasts and other plastids. Nat. Rev. Mol. Cell Biol. **14:** 787–802.

Kadirjan-Kalbach, D.K., Yoder, D.W., Ruckle, M.E., Larkin, R.M., and Osteryoung, K.W. (2012). FtsHi1/ARC1 is an essential gene in Arabidopsis that links chloroplast biogenesis and division. Plant J. **72:** 856–867.

Kasmati, A.R., Töpel, M., Patel, R., Murtaza, G., and Jarvis, P. (2011). Molecular and genetic analyses of Tic20 homologues in *Arabidopsis thaliana* chloroplasts. Plant J. **66:** 877–889.

Keegstra, K., and Yousif, A.E. (1986). Isolation and characterization of chloroplast envelope membranes. Methods Enzymol. **118:** 316–325.

Kessler, F., and Blobel, G. (1996). Interaction of the protein import and folding machineries of the chloroplast. Proc. Natl. Acad. Sci. USA **93:** 7684–7689.

Kikuchi, S., Hirohashi, T., and Nakai, M. (2006). Characterization of the preprotein translocon at the outer envelope membrane of chloroplasts by blue native PAGE. Plant Cell Physiol. **47:** 363–371.

Kikuchi, S., Oishi, M., Hirabayashi, Y., Lee, D.W., Hwang, I., and Nakai, M. (2009). A 1-megadalton translocation complex containing Tic20 and Tic21 mediates chloroplast protein import at the inner envelope membrane. Plant Cell **21:** 1781–1797.

Kikuchi, S., Bédard, J., and Nakai, M. (2011). One- and two-dimensional blue native-PAGE and immunodetection of low-abundance chloroplast membrane protein complexes. Methods Mol. Biol. **775:** 3–17.

Kikuchi, S., Bédard, J., Hirano, M., Hirabayashi, Y., Oishi, M., Imai, M., Takase, M., Ide, T., and Nakai, M. (2013). Uncovering the protein translocon at the chloroplast inner envelope membrane. Science **339:** 571–574.

LaConte, L.E.W., Srivastava, S., and Mukherjee, K. (2017). Probing protein kinase-ATP interactions using a fluorescent ATP analog. Methods Mol. Biol. **1647:** 171–183.

Laustsen, P.G., Vang, S., and Kristensen, T. (2001). Mutational analysis of the active site of human insulin-regulated aminopeptidase. Eur. J. Biochem. **268:** 98–104.

Lee, Y.J., Kim, D.H., Kim, Y.-W., and Hwang, I. (2001). Identification of a signal that distinguishes between the chloroplast outer envelope membrane and the endomembrane system in vivo. Plant Cell **13:** 2175–2190.

Liu, L., McNeilage, R.T., Shi, L.X., and Theg, S.M. (2014). ATP requirement for chloroplast protein import is set by the Km for ATP hydrolysis of stromal Hsp70 in *Physcomitrella patens*. Plant Cell **26:** 1246–1255.

Lu, X., Zhang, D., Li, S., Su, Y., Liang, Q., Meng, H., Shen, S., Fan, Y., Liu, C., and Zhang, C. (2014). FtsHi4 is essential for embryogenesis due to its influence on chloroplast development in Arabidopsis. PLoS One **9:** e99741.

Matyskiela, M.E., Lander, G.C., and Martin, A. (2013). Conformational switching of the 26S proteasome enables substrate degradation. Nat. Struct. Mol. Biol. **20:** 781–788.

Meinke, D. (2013). Large-scale mutant analysis of seed development in Arabidopsis. In Seed Genomics, P.W. Becraft, ed (Ames, Iowa: Wiley-Blackwell), pp. 5–20.

Nakai, M. (2015a). The TIC complex uncovered: The alternative view on the molecular mechanism of protein translocation across the inner envelope membrane of chloroplasts. Biochim. Biophys. Acta **1847:** 957–967.

Nakai, M. (2015b). YCF1: a green TIC: Response to the de Vries et al. commentary. Plant Cell **27:** 1834–1838.

Nakai, M. (2018). New perspectives on chloroplast protein import. Plant Cell Physiol. **59:** 1111–1119.

Nickelsen, J. (2005). Cell biology: The green alga *Chlamydomonas reinhardtii*–A genetic model organism. Prog. Bot. **66:** 68–89.

Nielsen, E., Akita, M., Davila-Aponte, J., and Keegstra, K. (1997). Stable association of chloroplastic precursors with protein translocation complexes that contain proteins from both envelope membranes and a stromal Hsp100 molecular chaperone. EMBO J. **16:** 935–946.

Notredame, C., Higgins, D.G., and Heringa, J. (2000). T-Coffee: A novel method for fast and accurate multiple sequence alignment. J. Mol. Biol. **302:** 205–217.

Okuno, T., and Ogura, T. (2013). FtsH protease-mediated regulation of various cellular functions. Subcell. Biochem. **66:** 53–69.

Paila, Y.D., Richardson, L.G.L., and Schnell, D.J. (2015). New insights into the mechanism of chloroplast protein import and its integration with protein quality control, organelle biogenesis and development. J. Mol. Biol. **427:** 1038–1060.

Parker, N., Wang, Y., and Meinke, D. (2016). Analysis of Arabidopsis accessions hypersensitive to a loss of chloroplast translation. Plant Physiol. **172:** 1862–1875.

Patron, M., Sprenger, H.-G., and Langer, T. (2018). m-AAA proteases, mitochondrial calcium homeostasis and neurodegeneration. Cell Res. **28:** 296–306.

Puchades, C., Rampello, A.J., Shin, M., Giuliano, C.J., Wiseman, R.L., Glynn, S.E., and Lander, G.C. (2017). Structure of the mitochondrial inner membrane AAA+ protease YME1 gives insight into substrate processing. Science **358:** eaao0464.

Richardson, L.G.L., Singhal, R., and Schnell, D.J. (2017). The integration of chloroplast protein targeting with plant developmental and stress responses. BMC Biol. **15:** 118.

Ronquist, F., Teslenko, M., van der Mark, P., Ayres, D.L., Darling, A., Höhna, S., Larget, B., Liu, L., Suchard, M.A., and Huelsenbeck, J.P. (2012). MrBayes 3.2: efficient Bayesian phylogenetic inference and model choice across a large model space. Syst. Biol. **61:** 539–542.

Saikawa, N., Ito, K., and Akiyama, Y. (2002). Identification of glutamic acid 479 as the gluzincin coordinator of zinc in FtsH (HflB). Biochemistry **41:** 1861–1868.

Samson, F., Brunaud, V., Balzergue, S., Dubreucq, B., Lepiniec, L., Pelletier, G., Caboche, M., and Lecharny, A. (2002). FLAGdb/FST: a database of mapped flanking insertion sites (FSTs) of *Arabidopsis thaliana* T-DNA transformants. Nucleic Acids Res. **30:** 94–97.

Sauer, R.T., and Baker, T.A. (2011). AAA+ proteases: ATP-fueled machines of protein destruction. Annu. Rev. Biochem. **80:** 587–612.

Schnell, D.J., Kessler, F., and Blobel, G. (1994). Isolation of components of the chloroplast protein import machinery. Science **266:** 1007–1012.

Schreier, T.B., Cléry, A., Schläfli, M., Galbier, F., Stadler, M., Demarsy, E., Albertini, D., Maier, B.A., Kessler, F., Hörtensteiner, S., Zeeman, S.C., and Kötting, O. (2018). Plastidal NAD-dependent malate dehydrogenase: a moonlighting protein involved in early chloroplast development through its interaction with an FtsH12-FtsHi protease complex. Plant Cell **30:** 1745–1769.

Scott, S.V., and Theg, S.M. (1996). A new chloroplast protein import intermediate reveals distinct translocation machineries in the two envelope membranes: energetics and mechanistic implications. J. Cell Biol. **132:** 63–75.

Shi, L.X., and Theg, S.M. (2013). Energetic cost of protein import across the envelope membranes of chloroplasts. Proc. Natl. Acad. Sci. USA **110:** 930–935.

Sjögren, L.L., Tanabe, N., Lymperopoulos, P., Khan, N.Z., Rodermel, S.R., Aronsson, H., and Clarke, A.K. (2014). Quantitative analysis of the chloroplast molecular chaperone ClpC/Hsp93 in Arabidopsis reveals new insights into its localization, interaction with the Clp proteolytic core, and functional importance. J. Biol. Chem. **289:** 11318–11330.

Sokolenko, A., Pojidaeva, E., Zinchenko, V., Panichkin, V., Glaser, V.M., Herrmann, R.G., and Shestakov, S.V. (2002). The gene complement for proteolysis in the cyanobacterium *Synechocystis* sp. PCC 6803 and *Arabidopsis thaliana* chloroplasts. Curr. Genet. **41:** 291–310.

Stamatakis, A. (2014). RAxML version 8: a tool for phylogenetic analysis and post-analysis of large phylogenies. Bioinformatics **30:** 1312–1313.

Su, P.H., and Li, H.M. (2010). Stromal Hsp70 is important for protein translocation into pea and Arabidopsis chloroplasts. Plant Cell **22:** 1516–1531.

Sun, Q., Zybailov, B., Majeran, W., Friso, G., Olinares, P.D., and van Wijk, K.J. (2009). PPDB, the Plant Proteomics Database at Cornell. Nucleic Acids Res. **37:** D969–D974.

Svab, Z., and Maliga, P. (1993). High-frequency plastid transformation in tobacco by selection for a chimeric aadA gene. Proc. Natl. Acad. Sci. USA **90:** 913–917.

Tanabe, A.S. (2007). KAKUSAN: a computer program to automate the selection of a nucleotide substitution model and the configuration of a mixed model on multilocus data. Mol. Ecol. Notes **7:** 962–964.

Theg, S.M., Bauerle, C., Olsen, L.J., Selman, B.R., and Keegstra, K. (1989). Internal ATP is the only energy requirement for the translocation of precursor proteins across chloroplastic membranes. J. Biol. Chem. **264:** 6730–6736.

Wagner, R., Aigner, H., and Funk, C. (2012). FtsH proteases located in the plant chloroplast. Physiol. Plant. **145:** 203–214.

White, S.R., and Lauring, B. (2007). AAA+ ATPases: achieving diversity of function with conserved machinery. Traffic **8:** 1657–1667.

Witte, C.P., Noël, L.D., Gielbert, J., Parker, J.E., and Romeis, T. (2004). Rapid one-step protein purification from plant material using the eight-amino acid StrepII epitope. Plant Mol. Biol. **55:** 135–147.